ELSEVIER

Mechanics of Materials 31 (1999) 831–860

MECHANICS OF MATERIALS

www.elsevier.com/locate/mechmat

Gradient concepts for evolution of damage

Thomas E. Lacy [a,*], David L. McDowell [b], Ramesh Talreja [c]

[a] *Department of Aerospace Engineering, Wichita State University, Wichita, KS 67260-0044, USA*
[b] *G.W. Woodruff School of Mechanical Engineering, Georgia Institute of Technology, Atlanta, GA 30332-0405, USA*
[c] *D. Guggenheim School of Aerospace Engineering, Georgia Institute of Technology, Atlanta, GA 30332-0150, USA*

Received 7 July 1998; received in revised form 12 April 1999

Abstract

While low-order measures of damage have sufficed to describe the stiffness of bodies with distributed voids or cracks, such as the void volume fraction or the crack density tensor of Vakulenko, A.A., Kachanov, M., 1971. [Inz. AN SSSR., Mekhanika Tverdogo Tela (Mech. Solids) 6 (4), 159], addressing the growth of distributed defects demands a more comprehensive description of the details of defect configuration and size distribution. Moreover, interaction of defects over multiple length scales necessitates a methodology to sort out the change of internal structure associated with these scales. To extend the internal state variable approach to evolution, we introduce the notion of multiple scales at which first and second nearest-neighbor effects of nonlocal character are significant, similar to homogenization theory. Further, we introduce the concept of a cutoff radius for nonlocal action associated with a representative volume element (RVE), which exhibits statistical homogeneity of the evolution, and flux of damage gradients averaged over multiple subvolumes. In this way, we enable a local description at length scales below the RVE. The mean mesoscale gradient is introduced to reflect systematic differences in size distribution and position of damage entities in the evolution process. When such a RVE cannot be defined, the evolution is inherently statistically inhomogeneous at all scales of reasonable dimension, and the concept of macroscale gradients of internal variables is the only recourse besides micromechanics. Based on a series of finite element calculations involving evolution of 2D cracks in brittle elastica arranged in random periodic arrays, we examine the evolution of the mean mesoscale gradients and note some preliminary implications for the utility of such an approach.

1. Introduction

Continuum damage mechanics (CDM) provides a framework for the development of constitutive equations and damage evolution equations for defected solids. First introduced in the classical studies of creep rupture in metals by Kachanov (1958) and Rabotnov (1963), CDM is based on the thermodynamics of irreversible processes (Kestin, 1966; Kestin and Rice, 1970; Rice, 1971), internal state variable (ISV) theory (Coleman and Gurtin, 1967), and relevant physical considerations (assumption of distributed damage, homogenization concepts, definition of the damage variable, formulation of kinetic laws for damage evolution, etc.; cf. Krajcinovic (1989, 1996a), for excellent literature reviews of CDM). A solid that is highly heterogeneous at the mesoscale is considered an effective homogeneous continuum at the macroscale. Adopting the postulate of local action at the representative volume element (RVE) scale greatly simplifies the governing equations for boundary

* Corresponding author. Tel.: +1-316-978-6354.
E-mail address: lacy@ae.twsu.edu (T.E. Lacy)

0167-6636/99/$ - see front matter
PII: S0167-6636(99)00029-0

value problems, of course, relative to fully nonlocal theories. Macroscopic damage variables are judiciously selected to reflect the effects of mesostructural level irreversible processes on macroscale material behavior. Such damage descriptors may be obtained through a "low-order" homogenization (spatial average) of individual damage entities, neglecting details of the distribution of damage throughout the RVE. The fact that the theory refers to an homogeneous continuum, however, presents a serious obstacle in the development of damage evolution laws that incorporate effects of the heterogeneity of the solid at the mesoscale. Whereas effective moduli are somewhat insensitive to the distribution of microcracks, damage evolution is highly dependent on the local fluctuations in crack arrangement within the RVE used for stiffness calculations (cf. Kachanov, 1994). Bazant and Chen (1997) discuss the scale dependence of energy release in fracture of heterogeneous, quasi-brittle solids. In the homogenization process, critical information regarding the largest flaw size, minimum distance between flaws, and distribution of damage within an RVE is irrevocably lost. Such information is crucial to the development of viable evolution equations. Current CDM approaches have been generally limited to the case of dilute (noninteracting) damage. This limitation suggests the need for a higher-order continuum description of damage that retains key aspects of the damage distribution within an RVE. This work attempts to clarify key issues associated with the development of such a higher-order continuum formulation for evolution of damage. The specific case of brittle microcracked solids is examined in view of its long history of attention from the perspective of effective properties (cf. Budiansky and O'Connell, 1976; Kachanov, 1994; Krajcinovic, 1989, 1996a; Mura, 1991; Nemat-Nasser and Hori, 1993). This study will focus on isothermal, purely mechanical applications.

2. Implementation of CDM

2.1. Selection of damage variable

The selection of a macroscopic damage variable may, in principle, be somewhat arbitrary and often does not necessarily directly reflect any of the underlying dissipative or energy transfer processes occurring at the mesoscale. Commonly, a damage parameter is selected that can be expressed in terms of macroscopically measurable quantities (giving rise to so-called "effective-stress" or similar models). Numerous damage models have incorporated scalar or tensorial damage variables that can be characterized at the macroscale, for example, by change in compliance (cf. Chaboche, 1984). An alternative choice of damage variable is one that incorporates salient aspects of damage morphology in its definition. Such "micromechanically-inspired" damage models involving scalar, tensor, or "fabric tensor" representations of damage have been introduced in the study of heterogeneous materials containing voids or various crack-like surface discontinuities (cf. Onat and Leckie, 1988; Talreja, 1989, 1991; Nemat-Nasser and Hori, 1993; Kachanov, 1994; Krajcinovic, 1996a).

Either choice of damage parameter has inherent limitations that affect its utility in a CDM formulation. In general, both macroscopically measurable and micromechanically inspired damage variables neglect the varying effects of nonlocal or "nearest neighbor" influences (e.g., shielding and enhancement associated with adjacent flaws) that are essential to formulate damage evolution laws. Inclusion of such effects represents, perhaps, one of the greatest challenges in the development of a robust CDM formulation. For these reasons, more careful consideration of appropriate ISV measures of damage is warranted.

2.2. RVE definition and statistically homogeneous (SH) response functions

The aforementioned damage descriptors may be obtained through a spatial average of key features of individual damage entities contained within a suitably chosen observation window. Summarizing the work of Hill (1967), Hashin (1983), Nemat-Nasser and Hori (1993), and Krajcinovic (1996a,b), the RVE is commonly defined as a cube of material with dimension, L_{RVE}, subject to the following conditions (Krajcinovic, 1996a,b):

$$\frac{d}{L_{\mathrm{RVE}}} \ll 1, \quad L_{\mathrm{C}} \leqslant L_{\mathrm{RVE}} \leqslant L,$$
$$\left|\frac{\partial \sigma_{ij}^{0}}{\partial x_k}\right| L_{\mathrm{RVE}} \ll |\sigma_{ij}^{0}|, \tag{1}$$

where d is the characteristic size of microconstituents, L_{C} is the heterogeneity correlation length, L is a characteristic macroscopic structural dimension, $\boldsymbol{\sigma}^0$ is the mean field (volume averaged) stress, and (x_1, x_2, x_3) are the components of a Cartesian basis. Here d may also be interpreted as the wavelength over which the traction or displacement on the RVE boundary fluctuate about some mean value under conditions of uniform displacement or traction, respectively (Hashin, 1983). Statistical homogeneity, for general purposes, requires that all response functions of interest at the scale of the observation volume window (Helmholtz free energy, ψ; Cauchy stress tensor, $\boldsymbol{\sigma}$; small strain tensor, $\boldsymbol{\varepsilon}$; stiffness tensor, $\boldsymbol{C}$; etc.) are essentially invariant with respect to window position (cf. Hashin, 1983; Nemat-Nasser and Hori, 1993; Krajcinovic, 1996b; Alzebdeh et al., 1997). Note that statistical homogeneity of elastic moduli, such that $\boldsymbol{C}$ is relatively independent of whether uniform traction or uniform displacement is applied to the observation window boundary, is a somewhat more restrictive requirement than statistical homogeneity of field quantities (e.g., $\boldsymbol{\sigma}$, $\boldsymbol{\varepsilon}$). Ostoja-Starzewski and Wang (1989), Alzebdeh et al. (1997), Ostoja-Starzewski (1997) and Ostoja-Starzewski et al. (1994) provide excellent discussions regarding the selection of suitable observation windows for averaging response functions as well as the influence of observation window boundary conditions (e.g., uniform versus "random-periodic" traction and displacement boundary conditions) on the statistical homogeneity of response functions for a given window size. A majority of the treatment in the literature addresses determination of the minimum observation window necessary for statistical homogeneity of elastic moduli, $(\mathrm{RVE})_{\mathrm{STIFFNESS}}$.

In general, individual response functions must be averaged over different observation windows (RVEs) in order to satisfy conditions of statistical homogeneity. If the initial observation window (Window A in Fig. 1) is of insufficient size, then none of the average response functions will satisfy conditions of translational invariance with respect to window origin coordinates. If the observation window is gradually increased, eventually it may be of sufficient size (e.g., Window B in Fig. 1) to permit evaluation of statistically homogeneous (SH) response functions (e.g., ψ, $\boldsymbol{\sigma}$, $\boldsymbol{\varepsilon}$, $\boldsymbol{C}$) that are relatively insensitive to the distribution of mesostructural constituents. Such an observation window, however, may be insufficient to characterize SH response functions pertaining to damage evolution (i.e., thermodynamic forces conjugate to selected ISVs, $\boldsymbol{Y}$; damage evolution equations,

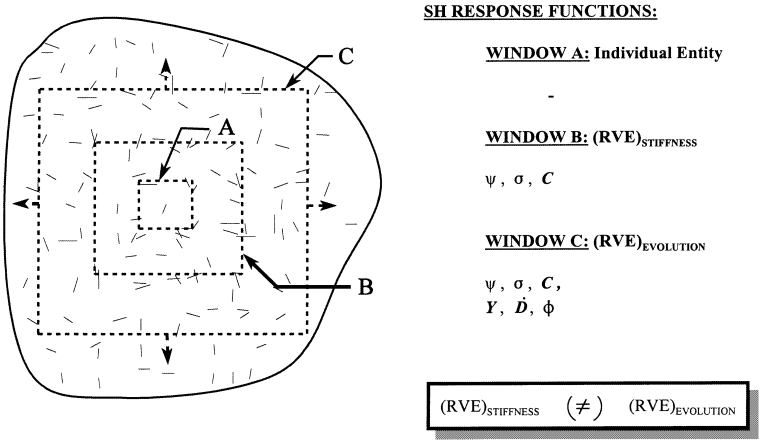

Fig. 1. RVE window size and statistically homogeneous (SH) response functions.

$\dot{\boldsymbol{D}}$; and dissipation potential, ϕ) that are governed by distribution characteristics of mesostructural entities. Based upon $(\mathrm{RVE})_{\mathrm{STIFFNESS}}$, many evolution processes are *statistically inhomogeneous* at the observation window scale (e.g., distributed crack growth in monolithics and composites, growth of void clusters or nonuniform size evolution of voids in ductile metals, texture evolution at the grain scale in polycrystals, etc.). Further, an $(\mathrm{RVE})_{\mathrm{EVOLUTION}}$ (Window C in Fig. 1) may not exist or may be of sufficient size to violate the third condition in Eq. (1), i.e.,

$$(\mathrm{RVE})_{\mathrm{EVOLUTION}} \neq (\mathrm{RVE})_{\mathrm{STIFFNESS}}. \tag{2}$$

In fact the notion of an $(\mathrm{RVE})_{\mathrm{EVOLUTION}}$ for SH response functions associated with damage evolution may not be meaningful in many practical cases. This is a key issue that is often overlooked in the literature, where the term "RVE" typically refers to the observation window necessary for stiffness characterization. This study aims to clarify issues associated with application of CDM to those practical scenarios where not all response functions satisfy statistical homogeneity. All future reference, unless otherwise noted, to "RVE" will denote $(\mathrm{RVE})_{\mathrm{STIFFNESS}}$, and all response functions will represent RVE-averaged quantities. Further, local quantities that vary spatially within the RVE will be denoted with a caret (e.g., $\hat{p}$).

3. 2D numerical simulation of evolving crack systems

In order to assess the viability of various macroscopic damage variables in a CDM formulation, parametric studies were performed to examine the effect of initial crack patterning on non-self-similar damage evolution for a number of arbitrary crack distributions in two-dimensional, idealized, brittle solids under plane strain conditions. Such an idealized problem was used to determine certain characteristic features and to clearly demonstrate the relevant issues, although it may be asserted that these features and issues pertain to much broader classes of damage in non-linear, history-dependent materials. The calculations were performed using the special purpose two-dimensional finite element code FRANC2D/L (cf. Bittencourt et al., 1996; James and Swensen, 1997). Lacy et al. (1997a,b) considered uniformly distributed doubly periodic crack distributions whereas this study focuses on arbitrary crack distributions. In each study, numerical simulations of evolving crack systems were conducted, and the RVE-averaged field quantities, elastic moduli, damage parameters and their associated conjugate thermodynamic forces were calculated at each increment of damage evolution. The reader is reminded that the term "RVE" as used herein denotes the observation window necessary for statistically homogeneous stiffness determination, $(\mathrm{RVE})_{\mathrm{STIFFNESS}}$; the condition for statistical homogeneity of elastic moduli was satisfied for each *initial* damage configuration considered. Three relatively simple damage parameters were considered in order to evaluate their utility in assessing damage evolution in arrays of flaws of various sizes and spatial distribution. These include:

(i) A damage variable that may be inferred from an effective stiffness tensor, analogous to that proposed by Chaboche (1984), with a component in the x_2-direction (see Fig. 2),

$$D_{\Delta E} = \frac{E_0 - E_2}{E_0} = \frac{\Delta E}{E_0}, \tag{3}$$

where E_2 and E_0 are Young's moduli in the x_2-direction for the damaged and virgin isotropic materials, respectively. The thermodynamic force component conjugate to $D_{\Delta E}$ (generalized energy release rate) may be expressed as

$$Y_{\Delta E} = -\rho \frac{\partial \psi}{\partial D_{\Delta E}} = -\rho \frac{\partial \psi}{\partial (\Delta E/E_0)}, \tag{4}$$

where ψ is the specific Helmholtz free energy and ρ is the mass density of the solid.

(ii) The 2D crack density tensor (cf. Vakulenko and Kachanov, 1971; Kachanov, 1980)

$$D_{ij} = \frac{1}{A} \sum_{k=1}^{N} a_k^2 n_i^k n_j^k, \tag{5}$$

where a_k is the half-length of the kth crack, A is the area of averaging, $\boldsymbol{n}^k$ is the unit vector normal to the kth crack, and N is the total number of cracks. The corresponding conjugate thermodynamic force to (5) is given by

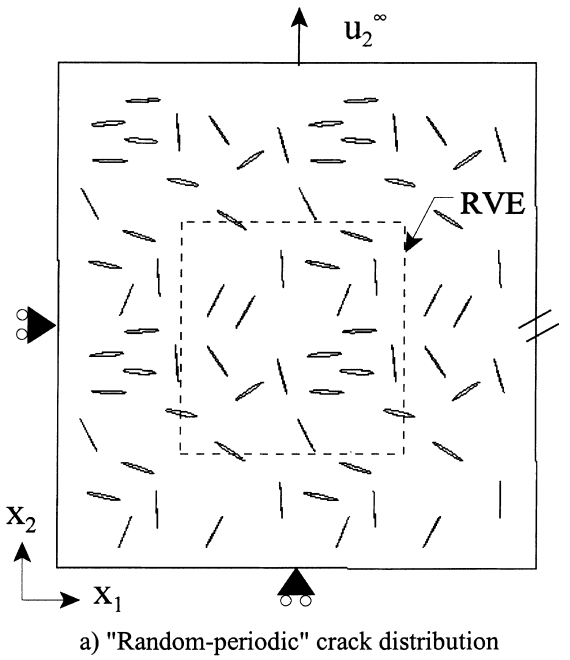

Fig. 2. Schematic of typical observation window and associated boundary conditions used in numerical simulations of damage evolution.

$$Y_{ij} = -\rho \frac{\partial \psi}{\partial D_{ij}} = -\rho \frac{\partial \psi}{\partial \left((1/A) \sum_{k=1}^{N} a_k^2 n_i^k n_j^k \right)}. \tag{6}$$

(iii) A scalar damage parameter based upon the total surface area of microcracks, i.e.,

$$D_A = \frac{1}{A} \sum_{k=1}^{N} a_k \tag{7}$$

and its corresponding thermodynamic force

$$Y_A = -\rho \frac{\partial \psi}{\partial D_A} = -\rho \frac{\partial \psi}{\partial \left((1/A) \sum_{k=1}^{N} a_k \right)}. \tag{8}$$

Eqs. (3)–(8) are representative low-order characterizations of damage. Eq. (3) may be determined from the damaged elastic modulus. The latter two "micromechanically-inspired" damage parameters may be evaluated from a knowledge of the characteristic defect distribution. For the idealized elastic-perfectly brittle materials considered in this study, $Y_{\Delta E}$, Y_{ij} and Y_A may be interpreted as the generalized strain energy release rate (ERR) associated with an increment of damage (evolution). It is recognized that a damage variable that is a linear function of the crack lengths in a given distribution will lead to relatively poor estimates of elastic moduli (cf. Kachanov, 1994); such a parameter (7) was included in this study in order to assess its utility in characterizing the ERR during distributed damage evolution. Note that irregularly spaced cracks will typically evolve in non-self-similar fashion. Thus, nonplanar cracks in the numerical simulations were idealized as slit cracks with identical crack tip coordinates in order to evaluate Eq. (5).

3.1. Key numerical results/observations

CDM is typically predicated on the assumption that an observation window, $(\mathrm{RVE})_{\mathrm{STIFFNESS}}$, exists that minimally ensures statistically homogeneous (SH) response functions pertaining to stiffness determination (e.g., $\boldsymbol{\sigma}$, $\boldsymbol{\varepsilon}$, and $\boldsymbol{C}$). This suggests that, to within an acceptable tolerance, these response functions should be unique functions of the damage variable used to characterize the degraded state of the material. In addition, CDM implicitly assumes that the RVE-averaged stiffness and response are invariant with respect to variations in microcrack sizes and number densities for which a given damage variable is fixed (Krajcinovic, 1996b).

Lacy (1998) showed that for the idealized case of uniformly distributed doubly periodic arrays of cracks, statistical *inhomogeneity* of response functions pertaining to stiffness determination (e.g., $\boldsymbol{\sigma}$, $\boldsymbol{\varepsilon}$, and $\boldsymbol{C}$) may arise even for the dilute damage case if crack interactions are significant. Accordingly, statistical homogeneity of such response functions is most likely if damage interactions are negligible or if the effects of crack shielding and enhancement tend to cancel each other when averaged over the observation window (cf. Kachanov, 1994). More importantly, Lacy (1998) demonstrated that use of certain low-order damage parameters such as those in Eqs. (3), (5), and (7) may result in response functions pertaining to *damage evolution* (i.e., threshold strain for evolution, and RVE-averaged ERR, $\boldsymbol{Y}$) that are *flaw size dependent even for dilute damage*. For a given damage state, $D_{\Delta E}$ (or D_{22}), an increment of damage extension $D_{\Delta E}$

(or D_{22}) during uniformly distributed damage evolution of a crack system with characteristic flaw size a_1 will produce more new crack surface area than an identical increment of damage extension for a second distribution with characteristic flaw size $a_2 > a_1$. This additional creation of crack surface area, for the dilute and noninteractive damage case, results in a higher RVE-averaged ERR, $Y_{\Delta E}$ (or Y_{22}), for the former distribution. This key point has been virtually overlooked in much of the CDM literature.

Lacy et al. (1997a,b) and Lacy (1998) confirmed that low-order damage descriptors such as (3), (5) and (7) are incapable of distinguishing between various crack distributions that produce markedly different global responses through an evolutionary process of damage. Lacy (1998) obtained *non-unique* results in the numerical evaluation of effective moduli, threshold strain for evolution, residual strength, and thermodynamic forces for different crack configurations with common values of $D_{\Delta E}$, D_{22}, or D_A; such results call into question the viability of such damage descriptors in addressing damage evolution of highly interactive crack systems in a CDM formulation. This was true even for cases where the effective moduli for each damage state were essentially statistically homogeneous with respect to a given window of observation, $(\mathrm{RVE})_{\mathrm{STIFFNESS}}$.

To illustrate this point, consider the following results. Fig. 2 shows a schematic of a representative model containing an arbitrary "random-periodic" distribution of cracks in an RVE consisting of an otherwise linearly elastic, isotropic, homogeneous solid. Periodic/symmetry boundary conditions were applied to simulate a repeating mesostructure. A far-field displacement, u_2^{∞}, was applied in the x_2-direction to the upper model boundary. The term "random-periodic" refers to the fact that the damage distribution is completely random within the RVE but is doubly periodic over the wavelength, L_{RVE} (cf. Ostoja-Starzewski et al., 1994; Alzebdeh et al., 1997; Ostoja-Starzewski, 1997). Such defects placed periodically about the RVE boundary serve to induce periodicity of field quantities along the RVE boundary as well as to minimize defect interaction with overall model boundaries; the choice of L_{RVE}, however, defines the length scales of material disorder (Alzebdeh et al., 1997). Incorporation of random periodic boundary condition results in statistical homogeneity of elastic moduli at lower number densities of heterogeneities than would be necessary when implementing other types of boundary conditions (Alzebdeh et al., 1997). Note that imposition of usual periodic boundary conditions (e.g., via multi-point constraint equations in finite element solutions) may lead to undesirable or aphysical interactions of defects with model boundaries. The material was assumed to have no intrinsic toughening capability, i.e., it was perfectly brittle. While it is recognized that such an assumption ignores the effect of material structure on evolution, the primary focus of the work was to establish a framework for addressing damage entity distribution effects on the evolution of damage, rather than to model the initiation and propagation of defects in actual brittle materials. While Lacy (1998) gives a detailed discussion of the numerical simulations of non-self-similar damage evolution, suffice it to say that the stress intensity factors K_{I}, K_{II} were determined at each increment and a mixed mode criterion suitable for propagation in brittle materials was employed.

Figs. 3 and 4 show the initial and final damage states associated with eight different random-periodic crack configurations used in the numerical simulations. It should be emphasized that each initial crack configuration satisfied conditions of statistical homogeneity of elastic moduli. Analysis of evolving random-periodic distributions consisting of both randomly oriented and parallel cracks was performed. In the following discussion, such crack configurations will be referred to as "random" and "random-parallel", respectively; it is understood that such designations refer to the distribution of damage within the RVE. The boundaries of the RVE for each case are denoted by the dashed lines in the figures. For a given realization of cracks, the initial crack center coordinates and orientation of individual cracks were random functions of position within the RVE subject to the condition that overlapping cracks were not permitted; for random-parallel crack distributions, all cracks were initially oriented perpendicular to the x_2-axis. Individual realiza-

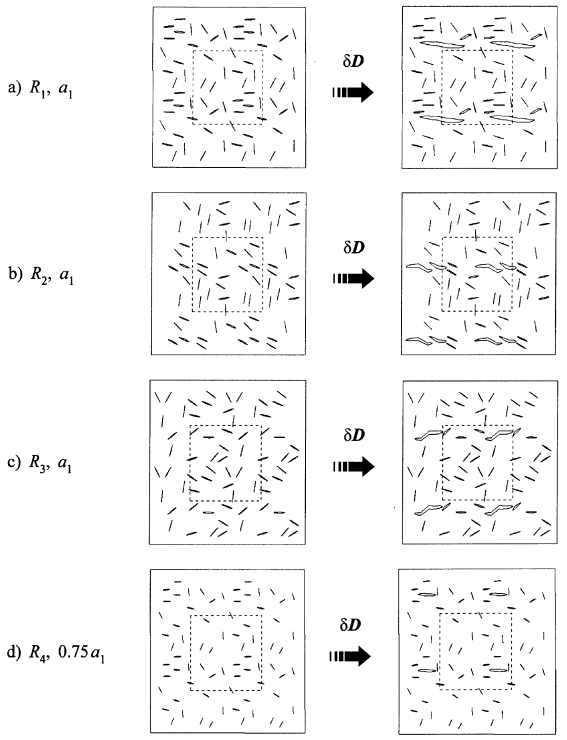

Fig. 3. Random-periodic crack distributions consisting of cracks with arbitrary crack center coordinates and crack orientations used in numerical simulations of damage evolution: (a) configuration R_1 ($a/L_{\mathrm{RVE}} = 0.08$); (b) configuration R_2 ($a/L_{\mathrm{RVE}} = 0.08$); (c) configuration R_3 ($a/L_{\mathrm{RVE}} = 0.08$); (d) configuration R_4 ($a/L_{\mathrm{RVE}} = 0.06$).

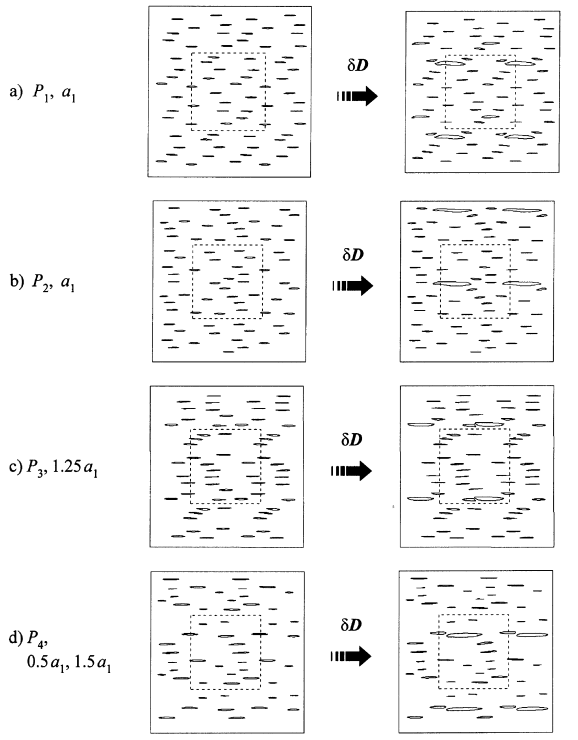

Fig. 4. Random-periodic crack distributions consisting of parallel cracks with arbitrary crack center coordinates used in numerical simulations of damage evolution: (a) configuration P_1 ($a/L_{\mathrm{RVE}} = 0.08$); (b) configuration P_2 ($a/L_{\mathrm{RVE}} = 0.08$); (c) configuration P_3 ($a/L_{\mathrm{RVE}} = 0.10$); (d) configuration P_4 ($a/L_{\mathrm{RVE}} = 0.04,\ 0.12$).

tions of random and random-parallel crack configurations will be designated by R_i and P_i, respectively, where $i = 1, \ldots, 4$. With the exception of the random-parallel crack configuration shown in Fig. 4(d), each of the configurations had a uniform initial crack length distribution, $(a_{\mathrm{inital}})_i$. Fig. 4(d) shows a random-parallel crack distribution consisting of cracks with two characteristic initial crack lengths. Key aspects associated with each initial crack configuration are summarized in Table 1. The numerical simulations for the random-periodic crack distributions were terminated prior to any crack coalescence. Crack kinking was permitted.

The initial damage configurations shown in Figs. 3 and 4 were selected to illustrate the effect of variable initial size and spatial distributions of defects on the subsequent evolution of randomly distributed cracks in brittle elastic solids. It is clear from the final damage states associated with each configuration shown in the figures that all cracks do not participate equally in the evolution process. Damage evolution for these random configurations consists of growth of a relatively few domi-

Table 1
RVE data for random-periodic crack arrays used in the numerical simulations

Case	Description	$a_{\mathrm{initial}}/L_{\mathrm{RVE}}$
1	Random (R_1)	0.08
2	Random (R_2)	0.08
3	Random (R_3)	0.08
4	Random(R_4)	0.06
5	Random-parallel (P_1)	0.08
6	Random-parallel (P_2)	0.08
7	Random-parallel (P_3)	0.10
8	Random-parallel (P_4)	0.04, 0.12

nant flaws within the RVE. In brittle elastic solids with no intrinsic toughening mechanisms, localized extension of preferentially arranged defects is to be expected considering local driving forces for evolution are largely dictated by local variations in the crack array geometry (cf. Kachanov, 1994). Note that for uniformly distributed doubly periodic crack distributions (cf. Lacy et al., 1997a), all the cracks evolve and actively contribute to the total energy dissipated during damage evolution. For these random distributions of cracks, however, only a select few defects contribute to the energy dissipated during evolution through their direct extension; the remainder of the cracks participate in the evolution process through their interactions (i.e., shielding or enhancement) as well as their contribution to stress redistribution (''load shedding'') within the RVE. Lacy (1998) demonstrated that for a random-periodic crack system subjected to uniaxial loading as shown in Fig. 2, it is reasonable to assume that the entire change in the free energy associated with an increment of the crack density tensor in Eq. (5) is attributable to δD_{22}.

Using the crack density tensor, Eq. (5), to characterize the damage state of the material, Figs. 5(a) and 6(a) show the degradation in normalized stiffness, E_2/E_0, versus damage data for each of the four random configurations (R_1, R_2, R_3, R_4) and random-parallel configurations (P_1, P_2, P_3, P_4), respectively. Note that the stiffness versus damage relationships, to within a reasonable tolerance, do not evolve away from statistical homogeneity (i.e., become configuration dependent) except at higher crack densities ($D_{22} > 0.16$; cf. Figs. 5(a) and 6(a)). These results are consistent with those obtained by Kachanov (1992, 1994) who observed that the effective moduli of solids containing randomly distributed, strongly interacting cracks are relatively insensitive to the distribution of cracks within a given material sample. The thermodynamic force conjugate to D_{22}, however, is markedly different for each distribution. Figs. 5(b) and 6(b) show that the normalized RVE-averaged ERR, $Y_{22}/(Y_{22})_{\mathrm{REF}}$, is a non-linear decreasing function of crack density and displays a strong characteristic crack size dependence. Here $(Y_{22})_{\mathrm{REF}}$ is a reference value associated with the initial damage state for a uniformly distributed doubly periodic crack distribution with an initial crack size $a_{\mathrm{initial}}/L_{\mathrm{RVE}} = 0.07$ (see Lacy, 1998). Similar to the results of Lacy et al. (1997a,b), the RVE-averaged ERR, Y_{22}, is significantly larger for the distributions containing smaller cracks than for those with larger initial characteristic crack sizes; Y_{22} also decreases more rapidly with increasing damage for these cases. It is likely that both the characteristic size of defects in a given distribution as well as the relative state of crack shielding or enhancement present in the vicinity of critical flaws influence the initial magnitude of Y_{22} for a given distribution as well as the trajectory of Y_{22} with increasing damage (cf. Lacy et al., 1997a,b; Lacy, 1998).

3.2. Implications for CDM

Considering that *all* the response functions of interest from the numerical simulations were evaluated over the observation window necessary for stiffness determination, $(\mathrm{RVE})_{\mathrm{STIFFNESS}}$, it is not surprising that response functions pertaining to *damage evolution* (i.e., threshold strain for evolution, and RVE-averaged ERR, $\boldsymbol{Y}$) are generally statistically *inhomogeneous* (configuration dependent) at this scale. It is tempting to assert that if these quantities are averaged over an observation window sufficiently enlarged relative to $(\mathrm{RVE})_{\mathrm{STIFFNESS}}$ then statistical homogeneity of evolution-related response functions would follow for the case of noninteractive damage. Recall, however, that the numerical results indicate that the thermodynamic forces conjugate to the selected damage ISVs are *flaw size dependent even for dilute damage*. While the response functions related to stiffness determination may be invariant with respect to variations in microcrack sizes and number densities for which a given damage variable in Eqs. (3), (5), and (7) is fixed, the same does not hold true for the response functions related to evolution. The existence of an observation window, $(\mathrm{RVE})_{\mathrm{EVOLUTION}}$, resulting in SH response functions pertaining to evolution is by no means assured for a given selection of damage parameter. Such an observation window, $(\mathrm{RVE})_{\mathrm{EVOLUTION}}$, did not exist for the brittle crack systems considered here; this is also likely the case for other

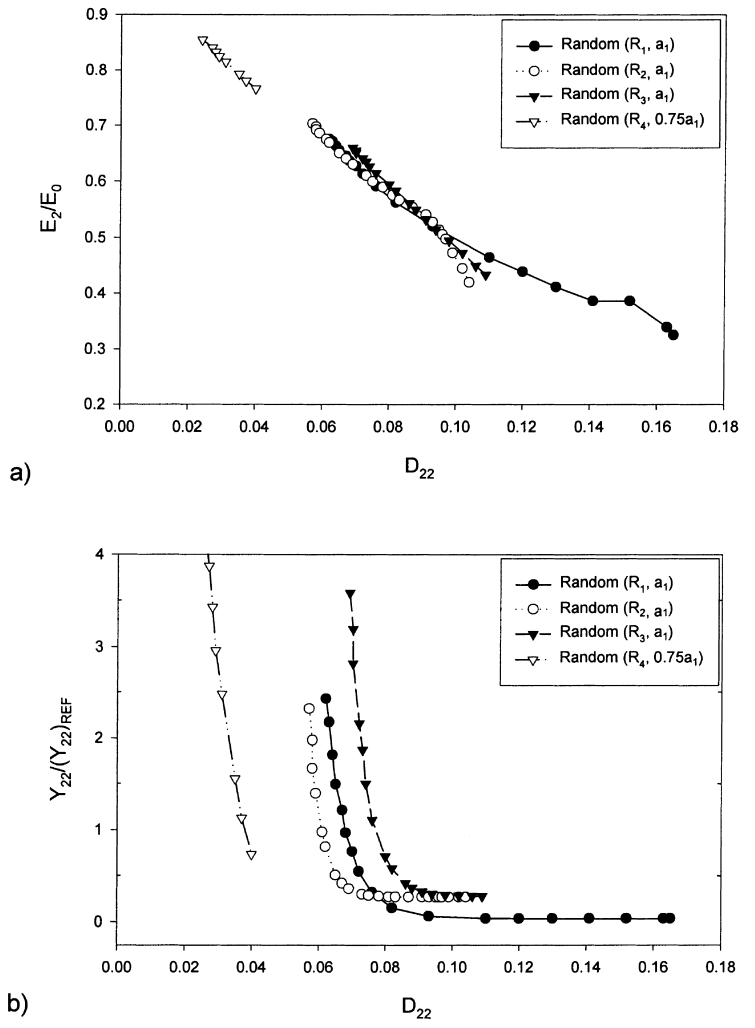

Fig. 5. (a) Normalized stiffness and (b) normalized thermodynamic force conjugate to D_{22} obtained from numerical simulations of damage evolution in random crack distributions.

realistic cases of materials sustaining various types of damage.

When attempting to extend CDM to those cases where the observation window, $(\mathrm{RVE})_{\mathrm{EVOLUTION}}$, either does not exist or is prohibitively large in comparison with $(\mathrm{RVE})_{\mathrm{STIFFNESS}}$, perhaps the only plausible option is to evaluate the response functions pertaining to evolution (i.e., threshold strain for evolution, and RVE-averaged ERR, $\boldsymbol{Y}$) using the observation window necessary for stiffness determination, $(\mathrm{RVE})_{\mathrm{STIFFNESS}}$, while acknowledging the lack of statistical homogeneity associated with these functions. Application of CDM to the statistically *inhomogeneous* case minimally requires the introduction of additional ISVs that account for the effect of the nonuniformity of the size and spatial distribution of damage within the RVE on the macroscale response. The evolution process will therefore depend on the initial configuration of damage and associated initial conditions on the damage variable. Such a higher-order continuum framework remains largely undeveloped, especially within the context of statistical inhomogeneity outlined here. While such a higher-

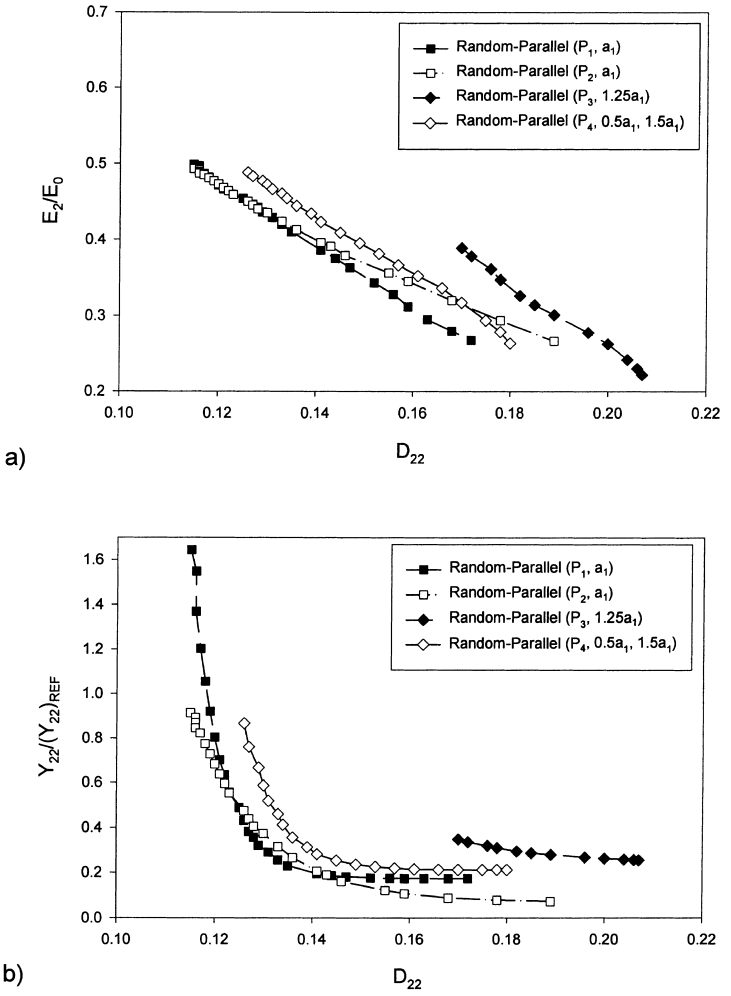

Fig. 6. (a) Normalized stiffness and (b) normalized thermodynamic force conjugate to D_{22} obtained from numerical simulations of damage evolution in random-parallel crack distributions.

order description may be possible using transmission factors (Kachanov, 1987, 1992, 1994) or other such approaches that can be obtained from detailed micromechanical analyses of the RVE, one goal of a CDM approach is to suggest relatively straightforward geometric descriptors that do not require large scale many-body numerical calculations and associated evolution of interactions in their formulation. In the remainder of this paper, preliminary concepts are outlined which may prove useful in the development of appropriate higher-order damage descriptors for use in a CDM approach.

4. Elements of a higher-order continuum formulation

The preceding numerical simulations suggest that damage evolution in perfectly brittle materials with randomly distributed cracks involves a relatively small fraction of preferentially arranged defects within the RVE used for stiffness determination. Crack extension in this case is limited to a number of *active* subvolumes within the RVE, the location of which depends on the mesoscale distribution of defects as well as the nature and severity of crack interactions. The nonuniformity in

the distribution of damage evolution sites within the RVE, nonlocal influences associated with crack interactions, and inherent statistical inhomogeneity of evolution-related response functions associated with use of damage variables with an intrinsic flaw size dependence all pose serious obstacles to the application of CDM to characterize the evolution of distributed crack systems in brittle materials. The fact that damage evolution within active subvolumes of the RVE depends on the distribution of mesoscale constituents leads logically to consideration of various nonlocal/gradient theories.

In order to facilitate the following discussion of physical phenomena manifested at fundamentally different spatial scales, it is useful to introduce several concepts pertaining to the observation scale necessary to characterize a particular deformation process. Adopting a notion of various observation scales similar to that of Krajcinovic (1996a), the *mesoscale* refers to the range of lengths over which the solid is heterogeneous and piecewise continuous. Individual geometric features of the mesostructure (e.g., microcracks, voids, fibers, inclusions, grains, etc.) are clearly recognizable. The deformation patterns are strongly influenced by the presence of heterogeneities at this scale and may be characterized using a *mesoscale coordinate system*, $\hat{\boldsymbol{x}}$ (cf. Fig. 7). In contrast, the *macroscale* refers to the range of lengths over which the solid may be considered in some sense as an effective homogeneous continuum (e.g., the range of characteristic lengths that would exceed the RVE dimension, L_{RVE}); the discrete material structure and texture inherent at the mesoscale are smeared out at the macroscale. The deformation at this observation scale may be characterized using the *macroscale coordinate system*, $\boldsymbol{x}$ (also shown in Fig. 7).

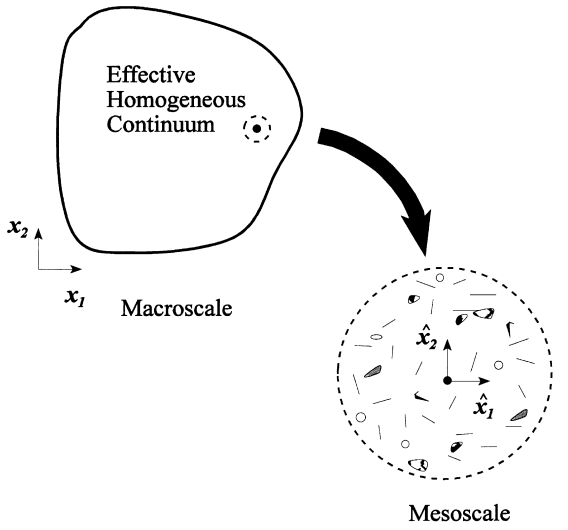

Fig. 7. Macroscopic and mesoscopic observation scales.

4.1. Nonlocal and gradient approaches

In typical nonlocal approaches, one or more of the macroscale governing equations involve integrals of state variables as functions of space or time (cf. Eringen, 1966; Kroner, 1967; Edelen, 1976; Pijaudier-Cabot and Bazant, 1987; Bazant, 1994). These integral expressions generally involve an *infinitely* extended zone of nonlocal action and may be approximated by truncated Taylor series expansions, giving rise to so-called macroscale *strain gradient* theories (cf. Mulhaus and Aifantis, 1991; Aifantis, 1992, 1994, 1995; Peerlings et al., 1996). Strain gradient approaches typically retain terms in the governing equations involving products of higher-order deformation gradients with coefficients whose magnitudes ostensibly reflect normalization by characteristic microstructural lengths associated with the nonlocal continuum. These terms are often introduced to regularize the boundary value problem characterizing deformation in the strain softening regime and require additional boundary conditions involving the gradients that lack a clear physical interpretation (cf. Peerlings et al., 1996).

Macroscale *damage gradient* approaches attempt to account for the effect of a nonuniform macroscale damage distribution on the macroscale response by assuming that the thermoelastic Helmholtz free energy depends not only on the macroscopic (RVE-averaged) ISV associated with damage, $\boldsymbol{D}$, but also on its macroscopic spatial gradient, $\nabla\boldsymbol{D}$, (cf. Markov, 1995; Fremond and Nedjar, 1996), i.e.,

$$\psi = \psi(\boldsymbol{\varepsilon}, T, \boldsymbol{D}, \nabla\boldsymbol{D}), \tag{9}$$

where $\boldsymbol{\varepsilon}$ is the small strain tensor, T is the absolute temperature. Generally, the state variables in damage gradient approaches are no longer independent; special care must be used to properly account for state variable coupling between $\boldsymbol{D}$ and $\nabla\boldsymbol{D}$ when applying the second law of thermodynamics. Apparently, in an attempt to address this issue, Fremond and Nedjar (1996) assumed that the dissipation associated with an increment of $\nabla\boldsymbol{D}$ was negligible.

Both strain gradient and damage gradient theories typically assume nonlocal continuum behavior at the *macroscale*. They generally focus on low-order measures of damage as well. In the presence of homogeneous macroscopic deformation or damage fields, these approaches result in governing equations that are consistent with those of a purely local continuum. In contrast, typical CDM approaches result in constitutive equations that satisfy the principle of local action at the *macroscale*. For a given value of a macroscopic damage variable, however, variations in the macroscale response functions associated with RVEs consisting of different distributions of defects are attributable to the differences in the size, orientation, and spatial distribution of defects within the RVEs, i.e., *the idealized continuum is nonlocal at the mesoscale*. This sub-RVE configuration dependence may manifest itself even in the presence of homogeneous far field deformation fields. Macroscale strain gradient or damage gradient approaches cannot capture this sub-RVE length scale effect. Moreover, nonlocal action dominantly occurs over finite sub-RVE length scales associated with defect clustering and nearest-neighbor interactions. For these reasons, the focus here is on constructing the structure of a nonlocal theory of CDM based on multiple scales of heterogeneity up to the order of the RVE dimension.

4.2. Characterization of mesostructural damage distribution

Damage ISVs should be judiciously selected to reflect the effects of mesoscale irreversible processes on macroscale material behavior. The goal in selection of a damage descriptor is to provide a physically meaningful, yet simple, macroscopic characterization of key mesoscale features of the solid. Such a descriptor should retain the *minimum* amount of information regarding the sub-RVE damage distribution necessary to characterize the problem and should, ideally, be amenable to direct quantification. Typical CDM approaches using ISV representations of damage have been deficient in this regard with some exceptions. Boyd (1992) retained a measure of mesoscale configuration to account for bending/extensional coupling within an RVE associated with damage distribution and Costanzo et al. (1996) used weighted shape functions to characterize the damage distribution in RVE subvolumes. In general, however, optimum RVE subvolume averaging procedures for damage evolution remain undeveloped.

Methods of spatial statistics (i.e., use of multivariate distribution functions) provide one possible framework for discriminating between different dispersions of damage entities within the RVE and specifying a purely geometric characterization of distribution effects (cf. Ripley, 1981; Stoyan et al., 1987; Stoyan and Stoyan, 1994). Such a formulation leads quite naturally to a purely geometric estimate of the RVE dimension, L_{RVE}, associated with long range order of the mesoscale damage distribution (cf. Pyrz, 1994). While such a characterization would facilitate the description of the alignment of crack-like features that lead to shielding or enhancement effects (cf. Gokhale, 1996), determination of appropriate forms for ISVs based upon such distribution functions remain undeveloped and no clear path is apparent. For example, characterization of stress redistribution with damage evolution is not directly reflected by evolving spatial statistics. For these reasons, use of spatial statistics is not considered as part this work in spite of the long range potential associated with such an approach. As an alternative, one may consider the use of *mesoscale* gradients to characterize the sub-RVE damage distribution.

4.2.1. Sub-RVE damage characterization using mesoscale gradients

Assuming that the ISVs used to characterize damage can be expressed as smoothly varying and continuous functions of position within the RVE,

the RVE-averaged damage variable, $\boldsymbol{D}$, can be expressed as a spatial average of the local (sub-RVE) values of the damage parameter, i.e.,

$$\boldsymbol{D} = \frac{1}{V_{\mathrm{RVE}}} \int_{V_{\mathrm{RVE}}} \hat{\boldsymbol{D}} \, \mathrm{d}V_{\mathrm{RVE}}, \tag{10}$$

where $\hat{\boldsymbol{D}}$ is the local (sub-RVE) value of the damage variable evaluated at a point, $\hat{\boldsymbol{x}}$, *within the RVE*. For nonuniform damage distributions, the local value of the damage parameter, $\hat{\boldsymbol{D}}$, will fluctuate about the mean (RVE-averaged) value, $\boldsymbol{D}$, throughout the RVE. Variations in the mesostructural distribution of damage entities will result in finite gradients in the local (sub-RVE) damage field, $\hat{\nabla}\hat{\boldsymbol{D}}$. Here the gradient operator, $\hat{\nabla}$, involves spatial derivatives at the *mesoscale*, i.e.,

$$\hat{\nabla} = \frac{\partial}{\partial \hat{x}_1}\hat{\boldsymbol{i}} + \frac{\partial}{\partial \hat{x}_2}\hat{\boldsymbol{j}} + \frac{\partial}{\partial \hat{x}_3}\hat{\boldsymbol{k}}, \tag{11}$$

where $\hat{\boldsymbol{i}}, \hat{\boldsymbol{j}}$, and $\hat{\boldsymbol{k}}$ are base vectors in the local (sub-RVE) coordinate system. It is essential to recognize that the gradient term in Eq. (9), $\nabla\boldsymbol{D}$, involves spatial derivatives with respect to *macroscale* coordinates (i.e., x_1, x_2, x_3); hence, the quantities $\nabla\boldsymbol{D}$ and $\hat{\nabla}\hat{\boldsymbol{D}}$ *involve fundamentally different length scales* akin to the use of multiple scales in the mathematical theory of homogenization of heterogenous media (cf. Sanchez-Palencia and Zaoui, 1987). Furthermore, if the distribution of defects is assumed to be random periodic, then there is no net flux of the mesoscale gradient of damage across the RVE boundary, i.e.,

$$\int_{S_{\mathrm{RVE}}} \hat{\nabla}\hat{\boldsymbol{D}} \cdot \hat{\boldsymbol{n}} \, \mathrm{d}S_{\mathrm{RVE}} \equiv \boldsymbol{0}. \tag{12}$$

Eq. (12) suggests that the nonlocal influence of mesoscale gradients manifests itself only within the RVE in the random periodic case.

Knowledge of mesoscale spatial gradients in the sub-RVE damage distribution may arguably be used to distinguish between different distributions of defects with the same value of RVE-averaged damage variable in Eq. (10). Andrieux et al. (1996) proposed a general framework based upon homogenization theory (cf. Sanchez-Palencia and Zaoui, 1987) for deriving constitutive equations at the *structure scale* ($L \gg L_{\mathrm{RVE}}$) for so-called generalized standard materials (Germain et al., 1983) incorporating sub-RVE spatial gradients of ISVs. Motivated by the work of Andrieux et al. (1996), this effort attempts to use mesoscale gradients of ISVs to characterize the damage entity distribution within the RVE.

A measure of the mesostructural variability within the RVE can be quantified using the absolute value of the mesoscale (sub-RVE) gradient of damage averaged over the RVE, i.e.,

$$\left|\overline{\frac{\partial \hat{\boldsymbol{D}}}{\partial \hat{x}_i}}\right| = \frac{1}{V_{\mathrm{RVE}}} \int_{V_{\mathrm{RVE}}} \left|\frac{\partial \hat{\boldsymbol{D}}}{\partial \hat{x}_i}\right| \mathrm{d}V_{\mathrm{RVE}}, \quad i = 1,2,3, \tag{13}$$

where an overbar is used to indicate the RVE-average of a mesoscale quantity, and it is understood that the derivatives in Eq. (13) operate on all components of the tensorial damage parameter $\hat{\boldsymbol{D}}$ (thus, the tensor $\hat{\nabla}\hat{\boldsymbol{D}}$ has a three-fold increase in rank over that of $\hat{\boldsymbol{D}}$). The RVE-averaged mesoscale gradient in Eq. (13) may be expressed in compact form as $\overline{\hat{\nabla}\hat{\boldsymbol{D}}}$, where

$$\overline{\hat{\nabla}\hat{\boldsymbol{D}}} \equiv \left|\overline{\frac{\partial \hat{\boldsymbol{D}}}{\partial \hat{x}_1}}\right|\hat{\boldsymbol{i}} + \left|\overline{\frac{\partial \hat{\boldsymbol{D}}}{\partial \hat{x}_2}}\right|\hat{\boldsymbol{j}} + \left|\overline{\frac{\partial \hat{\boldsymbol{D}}}{\partial \hat{x}_3}}\right|\hat{\boldsymbol{k}}. \tag{14}$$

4.3. ISVs based on mesoscale gradients of damage

4.3.1. Inclusion of higher-order ISVs in CDM formulation

The number and type of ISVs that must be retained in order to minimally characterize the macroscopic response of damaged solids largely depends on the problem to be solved. If the primary interest is determination of effective elastic moduli, then use of a low-order damage variable, $\boldsymbol{D}$, may be suitable for this purpose. When considering both stiffness reduction and damage evolution, however, inclusion of higher-order ISVs that retain information regarding the mesoscale configuration may be necessary, as suggested by the numerical simulations summarized in the previous section. The mean mesoscale gradient of damage in Eq. (14) provides one type of higher-order continuum description of the sub-RVE damage distribution. The components of $\overline{\hat{\nabla}\hat{\boldsymbol{D}}}$ may be used as additional ISVs to augment the

components of the low-order damage variable, $\boldsymbol{D}$, in a higher-order CDM formulation. In such an approach, the thermoelastic Helmholtz free energy may be expressed in terms of both sets of ISVs, i.e.,

$$\psi = \psi(\boldsymbol{\varepsilon}, T, \boldsymbol{D}, \overline{\hat{\nabla}\hat{\boldsymbol{D}}}). \tag{15}$$

Note that inclusion of the set $(\boldsymbol{D}, \overline{\hat{\nabla}\hat{\boldsymbol{D}}})$ in the constitutive equation (15) that are dependent on multiple varying spatial scales $(\boldsymbol{x}, \hat{\boldsymbol{x}})$ is a similar construct to that used in homogenization theory (cf. Sanchez-Palencia and Zaoui, 1987). With higher-order representations of damage such as Eq. (14), it is more likely that the theory will extrapolate to conditions not analyzed using low-order damage descriptors, such as evolution of nonuniformly distributed interactive crack systems with variable flaw size distributions. Moreover, such higher-order descriptors may even be useful in the presence of inelastic flow, time dependent deformation, or other deformation processes not amenable to detailed micromechanical analyses.

The inclusion of ISVs characterizing the mesoscale damage distribution complicates the formulation, particularly considering that the higher-order terms must be re-evaluated at every increment of damage. The total number of state variables may be reduced, however, if the mean *norm* of the mesoscale gradient associated with a given component of mesoscale damage is used as an ISV rather than the vector components themselves. For example, if a second rank tensor is used to characterize the damage distribution, the mean norm of the mesoscale gradient associated with the D_{22} component of damage is given by

$$\begin{aligned}\overline{\|\hat{\nabla}\hat{D}_{22}\|} &= \frac{1}{V_{\mathrm{RVE}}}\int_{V_{\mathrm{RVE}}}\left(\hat{\nabla}\hat{D}_{22}\cdot\hat{\nabla}\hat{D}_{22}\right)^{1/2}\mathrm{d}V_{\mathrm{RVE}} \\ &= \overline{\left(\hat{\nabla}\hat{D}_{22}\cdot\hat{\nabla}\hat{D}_{22}\right)^{1/2}}.\end{aligned} \tag{16}$$

Inclusion of mean mesoscale gradients as additional ISVs does not greatly alter the CDM formalism. The second law of thermodynamics for the case of evolving brittle damage may be expressed in terms of both sets of ISVs, i.e.,

$$-\rho\frac{\partial\psi}{\partial\boldsymbol{D}}\cdot\delta\boldsymbol{D} - \rho\lambda\frac{\partial\psi}{\partial\left(\overline{\hat{\nabla}\hat{\boldsymbol{D}}}\right)}\cdot\delta\left(\overline{\hat{\nabla}\hat{\boldsymbol{D}}}\right) \geqslant 0, \tag{17}$$

where a dot $(\cdot)$ denotes the scalar product of two tensors. The Lagrange multiplier, λ, is necessary because it cannot be a priori asserted that $\overline{\hat{\nabla}\hat{\boldsymbol{D}}}$ is independent of $\boldsymbol{D}$. The second term in Eq. (17) provides an estimate of the influence of the mesoscale damage configuration (i.e., size, orientation, and spatial distribution of defects within the RVE) on the total energy dissipated during damage extension. While the total energy dissipated during damage evolution must be non-negative, the potential coupling between state variables admits the possibility that the second term in Eq. (17) may be either positive or negative depending on the influence of mesoscale configuration. The dependence on damage gradients in the first term in Eq. (17) illustrates the influence of mesoscale configuration on the energy release associated with an increment of low-order damage variable, $\delta\boldsymbol{D}$; such dependence is essential to sort out differences between very short and very long crack lengths in a given distribution as well as the influence of defect interactions.

4.3.2. Practical considerations

The idealization of a smoothly varying and continuous mesoscale damage field, $\hat{\boldsymbol{D}}$, clearly breaks down as one transitions between progressively smaller spatial scales associated with the macro-, meso-, and microscales, respectively. Once the size of the heterogeneities at a given spatial scale reaches a certain fraction of the observation window size at that scale, then use of continuous functions to represent material structure becomes problematic. One may incorporate carefully chosen smoothing functions (cf. Nemat-Nasser and Hori, 1993) to locally smear out the effects of discrete material structure at a given scale or use basis functions (cf. Costanzo et al., 1996) to approximate the distribution of state variables within observation window subvolumes. As an alternative to either of these two approaches, one may characterize the sub-RVE damage distribution at a point within the RVE by simply considering the individual damage entities that fall within some finite RVE *subvolume* surrounding the point of interest.

Fig. 8 shows a schematic of an RVE consisting of a number of slit cracks in a two-dimensional

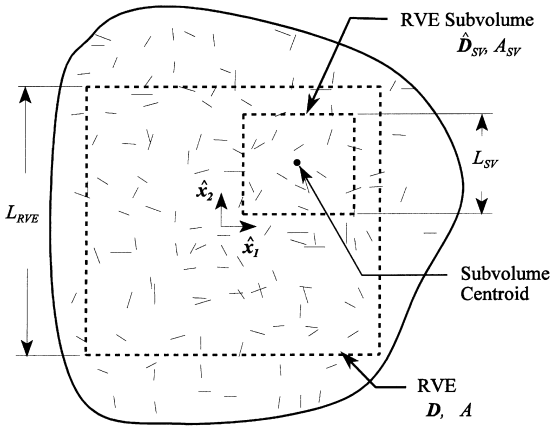

Fig. 8. Schematic of RVE and corresponding RVE subvolume for use in calculating mesoscale damage variables and mesoscale gradients.

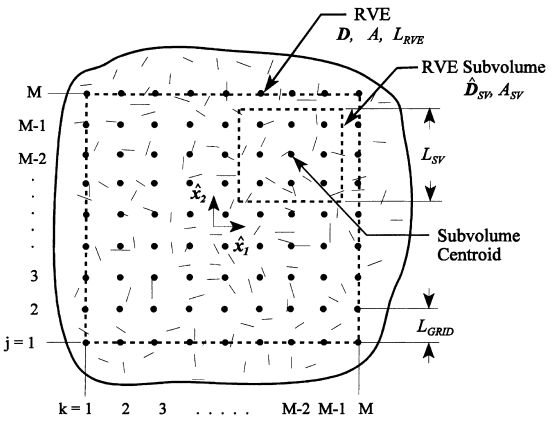

Fig. 9. Schematic of RVE and corresponding $M\times M$ grid of points for use in calculating mesoscale damage variables and mesoscale gradients.

solid. Consider a subvolume of material centered about an arbitrary point $(\hat{x}_1,\hat{x}_2)$ in the mesostructure and having dimension, L_{SV}, such that $L_{\mathrm{SV}} \leqslant L_{\mathrm{RVE}}$. A given mesoscale damage parameter, $\hat{\boldsymbol{D}}_{\mathrm{SV}}$, may be evaluated at the point $(\hat{x}_1,\hat{x}_2)$ in the RVE by averaging the effects of all the cracks that fall within the RVE subvolume surrounding the point (cf. Fig. 8), i.e.,

$$\hat{\boldsymbol{D}}_{SV} = \frac{1}{V_{\mathrm{SV}}}\int_{V_{\mathrm{SV}}} \eta\hat{\boldsymbol{D}}\,\mathrm{d}V_{\mathrm{SV}},$$
$$\frac{1}{V_{\mathrm{SV}}}\int_{V_{\mathrm{SV}}} \eta\,\mathrm{d}V_{\mathrm{SV}} = 1, \tag{18}$$

where V_{SV} is the volume of material contained in the RVE subvolume and η is a smoothing operator introduced to account for discrete mesostructure. The subvolume averaged quantity, $\hat{\boldsymbol{D}}_{\mathrm{SV}}$, reflects local smearing of structure and, to first order, may be used to approximate the discrete function, $\hat{\boldsymbol{D}}$, at point $(\hat{x}_1,\hat{x}_2)$ in the mesostructure. Thus, the variable $\hat{\boldsymbol{D}}$ will hereafter be used to denote $\hat{\boldsymbol{D}}_{\mathrm{SV}}$ for brevity. The subvolume centroid coordinates may be translated by some differential distance $(\delta\hat{x}_1,\ \delta\hat{x}_2)$ and the subvolume averaged damage parameter may be re-evaluated at the new subvolume location. This process may be repeated until the value of the mesoscale damage parameter is determined at a number of discrete points spanning the RVE. Fig. 9 shows an $M\times M$ square grid of points *uniformly* distributed throughout an RVE comprised of a number of slit cracks in a two-dimensional solid. Here the rows and columns of grid points are oriented such that they are parallel to the mesoscale coordinate axes, respectively, and have spacing, L_{GRID}. Once the value of the mesoscale damage parameter, $\hat{\boldsymbol{D}}$, has been determined at every grid point, the absolute value of the components of the mesoscale damage gradient, $\hat{\nabla}\hat{\boldsymbol{D}}$, at each grid point in the RVE may be approximated using three-point formulas (cf. Hoffman, 1992), i.e.,

$$\left|\frac{\partial\hat{\boldsymbol{D}}(\hat{x}_1,\hat{x}_2)}{\partial\hat{x}_1}\right| \approx \left|\frac{\hat{\boldsymbol{D}}(\hat{x}_1+L_{\mathrm{GRID}},\hat{x}_2)-\hat{\boldsymbol{D}}(\hat{x}_1-L_{\mathrm{GRID}},\hat{x}_2)}{2L_{\mathrm{GRID}}}\right|,$$
$$\left|\frac{\partial\hat{\boldsymbol{D}}(\hat{x}_1,\hat{x}_2)}{\partial\hat{x}_2}\right| \approx \left|\frac{\hat{\boldsymbol{D}}(\hat{x}_1,\hat{x}_2+L_{\mathrm{GRID}})-\hat{\boldsymbol{D}}(\hat{x}_1,\hat{x}_2-L_{\mathrm{GRID}})}{2L_{\mathrm{GRID}}}\right|. \tag{19}$$

If the components of the mesoscale damage gradient evaluated at a point corresponding to the jth row and kth column of grid points shown in Fig. 9 can be represented as $|\partial\hat{\boldsymbol{D}}(j,k)/\partial\hat{x}_i|$, then the components of the RVE-averaged mesoscale

gradient (14) for the two-dimensional case may be expressed as

$$\overline{\left|\frac{\partial \hat{\boldsymbol{D}}}{\partial \hat{x}_i}\right|} \approx \frac{1}{(M-1)^2}\sum_{j=1}^{M-1}\sum_{k=1}^{M-1}\left|\frac{\partial \hat{\boldsymbol{D}}(j,k)}{\partial \hat{x}_i}\right|, \quad i=1,2. \tag{20}$$

Here the range on the summation is $M-1$ because it is assumed that the distribution of defects is random periodic.

It is important to recognize that the subvolume averaged mesoscale damage variables are, by definition, statistically inhomogeneous for $L_{\mathrm{SV}} < L_{\mathrm{RVE}}$ and strongly depend on the choice of subvolume window size used for averaging. As the subvolume size, L_{SV}, approaches the RVE dimension, L_{RVE}, then $\hat{\boldsymbol{D}} \to \boldsymbol{D}$ and $\hat{\nabla}\hat{\boldsymbol{D}} \to \boldsymbol{0}$. Furthermore, if the subvolume dimension is smaller than the characteristic flaw size or minimum crack spacing, then the calculated values of mesoscale damage and damage gradients cease to represent averaging over a meaningful length scale. The mesoscale gradient is dependent on both the subvolume size, L_{SV}, and spacing between points used to evaluate the spatial derivatives, L_{GRID}. Minimally, the subvolume dimension should be somewhat larger than the grid spacing in order to ensure reasonably smooth varying estimates of the mesoscale damage and damage gradient distributions. This suggests that the mesoscale averaging procedure may be based on overlapping subvolumes (cf. Fig. 9). Additionally, in order to minimize the calculation of spurious gradients resulting from averaging over subvolumes containing no damage entities, use of a subvolume dimension greater than two times the mean center-to-center distance between cracks in a given distribution, $2d_{\mathrm{mean}}$, may be desirable; this suggests that *on average* each subvolume will contain at least one crack. Ideally, subvolume dimensions should be selected that allow for the calculation of meaningful gradients and *reflect averaging over appropriate finite zones of nonlocal action* within the RVE. In actual materials with microstructure, the optimum value of the grid spacing, L_{GRID}, used in the subvolume averaging procedure could likely be defined in terms of some characteristic microstructural dimension (average grain size, fiber diameter, etc.) while the subvolume dimension, L_{SV}, could ostensibly be specified in terms of an appropriate measure of the relative distribution of crack center coordinates within the RVE.

The mean mesoscale gradient in Eq. (20) provides an inherently nonlocal representation of the sub-RVE damage distribution manifested in the dependence of mesoscale gradients on the length scales associated with subvolume averaging, i.e., L_{SV} and L_{GRID}. Noting that a number of subvolume dimensions and grid spacings may be necessary in order to reflect averaging over finite zones of nonlocal action associated with first, second, etc., and nth nearest-neighbor crack interactions as well as defect clustering within the RVE, it may be argued that the nonlocal subvolume averaging technique advanced here admits a multitude of characteristic mesostructural lengths associated with the nonlocal mesostructure. Distributions of defects having multiple correlation lengths associated with defect clustering or variable size distributions of defects within an RVE may require use of variable subvolume dimensions in the sub-RVE averaging process in order to adequately characterize the mesoscale damage distribution, or perhaps introduction of gradients computed at P spatial scales, e.g., $(\hat{\nabla}\hat{\boldsymbol{D}})^{(1)}$, $(\hat{\nabla}\hat{\boldsymbol{D}})^{(2)}, \ldots$, and $(\hat{\nabla}\hat{\boldsymbol{D}})^{(P)}$ calculated based upon $(L_{\mathrm{SV}}^{(1)}, L_{\mathrm{GRID}}^{(1)})$, $(L_{\mathrm{SV}}^{(2)}, L_{\mathrm{GRID}}^{(2)}), \ldots$, and $(L_{\mathrm{SV}}^{(P)}, L_{\mathrm{GRID}}^{(P)})$, respectively. Properly chosen, values of L_{SV} may conceivably represent "cutoff"scales for the extent of nonlocal action within the RVE associated with various types of damage interactions. This is in contrast to typical gradient approaches that generally involve a single characteristic mesostructural length that enters the macroscale constitutive equations and implicitly assume an infinite extent of at least weak nonlocal action.

In this study, simulation of random-periodic boundary conditions led to SH response functions pertaining to stiffness determination using RVEs containing a relatively few number of cracks (e.g., $N \approx 18$). In order to fully assess the ability of the mesoscale averaging principles outlined here to distinguish between different crack systems with highly variable flaw size distributions and strong defect clustering within the RVE, however, it is desirable to consider RVEs containing signifi-

cantly larger numbers of cracks. Practical considerations dictate that such large scale numerical simulations may be best performed using a boundary element approach (cf. Brebbia et al., 1984), hybrid approach (cf. Annigeri and Cleary, 1984), robust singular integral technique (cf. Binienda et al., 1993), or other similar strategy that does not require the extensive remeshing associated with use of the finite element method to model distributed damage evolution. Use of two-point statistics (cf. Stoyan and Stoyan, 1994) to characterize the occurrence intensity of inter-entity distances may provide an ideal framework for assessing appropriate length scales for subvolume averaging. In addition, investigation of various nonlocal weight functions (cf. Bazant, 1994) for use in the subvolume averaging procedure may be warranted. These types of issues must be addressed in order to fully establish the mesoscale averaging principles outlined here.

4.4. Numerical evaluation of RVE-averaged mesoscale gradients

4.4.1. Determination of appropriate length scales for subvolume averaging

For the idealized perfectly brittle material considered in this study, no characteristic material dimension exists on which to base the grid spacing used in the subvolume averaging procedure. Hence, the only length scales on which to define L_{GRID} and L_{SV} are those associated with the crack distribution itself (normalized average crack size, $a_{\mathrm{ave}}/L_{\mathrm{RVE}}$, mean center-to-center crack spacing, $d_{\mathrm{mean}}/L_{\mathrm{RVE}}$, and minimum tip-to-tip distance between cracks, $d_{\mathrm{min}}/L_{\mathrm{RVE}}$, etc.). The mean crack spacing in a given distribution, to first order, may be estimated from the RVE dimension and total number of cracks, N, contained within the RVE, i.e.,

$$d_{\mathrm{mean}}/L_{\mathrm{RVE}} \approx N^{-1/2}. \tag{21}$$

While the approximation in Eq. (21) assumes a uniform distribution of cracks within the RVE, such a construct may prove useful in comparing various subvolume dimensions used in the calculation of mesoscale quantities.

Parametric studies were performed to determine the effect of various values of L_{SV} and L_{GRID} on the calculated mesoscale damage and damage gradient distributions, respectively, within an RVE corresponding to the initial damage state associated with random configuration (R_1) (cf. Fig. 3(a)). The magnitude of the fluctuations as well as the peak values in both the mesoscale damage and damage gradient distributions generally increased with decreasing grid spacing, L_{GRID}, and/or decreasing subvolume dimension, L_{SV}. A damage parameter based on the scalar crack density was used to characterize the RVE-averaged damage distribution, i.e.,

$$D_\rho = \frac{1}{A}\sum_{k=1}^{N} a_k^2. \tag{22}$$

A mesoscale damage variable analogous to Eq. (22) was used to characterize the sub-RVE damage distribution, i.e.,

$$\hat{D}_\rho = \frac{1}{A_{\mathrm{SV}}}\sum_{k=1}^{N} f_k a_k^2, \tag{23}$$

where $A_{\mathrm{SV}} = L_{\mathrm{SV}}^2$ is the averaging area in the RVE subvolume, and f_k is the fraction of the kth crack falling within a given subvolume. The absolute value of the mesoscale damage gradient, $|\partial \hat{D}_\rho/\partial \hat{x}_i|$, may be determined using Eqs. (23) and (19). For the two-dimensional case, the ith component of the mesoscale damage gradient vector may be expressed using shorthand notation as $|\hat{D}_{\rho,\hat{x}_i}|$, where it is understood that the comma notation implies differentiation with respect to the variable that follows it, i.e.,

$$\left|\hat{D}_{\rho,\ \hat{x}_i}\right| \equiv \left|\frac{\partial \hat{D}_\rho}{\partial \hat{x}_i}\right|. \tag{24}$$

For illustration purposes, Fig. 10 shows a three-dimensional mesh plot of the normalized sub-RVE damage distribution, $\hat{D}_\rho/D_\rho$, and normalized $\hat{x}_1$-component of mesoscale damage gradient, $|\hat{D}_{\rho,\hat{x}_1}|/D_\rho$, as a function of normalized position, $\hat{\boldsymbol{x}}/L_{\mathrm{RVE}}$, within an RVE corresponding to the initial damage state associated with random configuration (R_1). The mesoscale damage and damage gradient distributions shown in the figure were

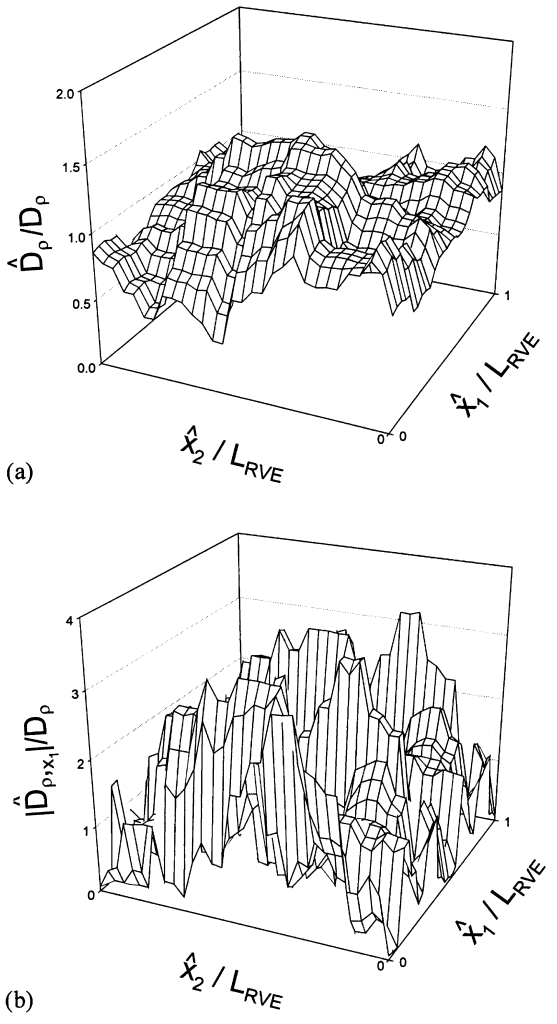

Fig. 10. (a) Mesoscale damage and (b) mesoscale damage gradient distributions based upon $L_{GRID}/L_{RVE} = 1/16$ and $L_{SV}/L_{RVE} = 1/2$.

calculated using a subvolume dimension, $L_{SV} \approx 2d_{mean}$, and grid spacing, $L_{GRID} \approx d_{min}$. Based upon the results of the parametric study, these values may serve to characterize the effects of first nearest-neighbor crack interactions using mesoscale damage gradients. Note that $L_{SV} = 2d_{mean}$ arguably reflects, in an average sense, the zone of nonlocal action associated with first nearest-neighbor crack interactions in a given distribution. For these reasons, a subvolume dimension, $L_{SV}/L_{RVE} = 1/2$ ($\approx 2d_{mean}/L_{RVE}$), and grid spacing, $L_{GRID}/L_{RVE} = 1/16$ ($\approx d_{min}$), were used to characterize the mean subvolume gradients for all the random and random-parallel crack distributions used in the numerical simulations of damage evolution.

Such a selection of the length scales for subvolume averaging is likely suitable for the perfectly random distributions of cracks considered in this study. If the distribution of crack centers in a given damage distribution is correlated, however, use of a subvolume dimension based on the approximation in Eq. (21) may be inappropriate. In the latter case, a subvolume dimension based on a more precise definition of mean crack spacing is likely more suitable.

4.4.2. Determination of mean mesoscale gradients for evolving crack systems

In order to calculate the evolving mean mesoscale gradient for each of the random-periodic crack distributions considered in this study, it was necessary to define *mesoscale* damage variables corresponding to Eqs. (3), (5), and (7), respectively:

(i) A scalar mesoscale damage variable based on the degraded elastic stiffness of the RVE subvolume corresponding to Eq. (3), i.e.,

$$\hat{D}_{\Delta E} = \frac{E_0 - \hat{E}_2}{E_0} = \frac{\Delta \hat{E}}{E_0}, \tag{25}$$

where $\hat{E}_2$ is the magnitude of the reduced Young's modulus in the direction of the applied loading averaged over the RVE subvolume. Note that Eq. (25) usually requires that computational micromechanics be used in order to estimate the mesoscale stiffness reduction associated with a given subvolume damage distribution. For this reason, calculation of mesoscale gradients based upon the degradation of sub-RVE elastic moduli, $\hat{D}_{\Delta E}$, was not considered as part of this study.

(ii) A mesoscale crack density tensor based upon the fraction of the total number of microcracks contained within a given RVE subvolume corresponding to Eq. (5), i.e.,

$$\hat{D}_{ij} = \frac{1}{A_{SV}} \sum_{k=1}^{N} f_k \; a_k^2 \; n_i^k n_j^k. \tag{26}$$

For the two-dimensional case, Eqs. (19) and (20) and a relation similar to Eq. (16) may be used to calculate the vector components and norm,

respectively, of the mean mesoscale gradient associated with each element of Eq. (26).

(iii) A scalar mesoscale damage parameter based upon the total surface area of microcracks contained within a given RVE subvolume analogous to Eq. (7), i.e.,

$$\hat{D}_A = \frac{1}{A_{SV}} \sum_{k=1}^{N} f_k a_k. \tag{27}$$

Again, Eqs. (19) and (20) and a relation similar to Eq. (16) may be used to calculate the vector components and norm, respectively, of the mean mesoscale gradient associated with Eq. (27).

The latter two mesoscale damage variables in Eqs. (26) and (27) may be evaluated from a knowledge of the crack array geometry.

Mean mesoscale gradients were calculated for each of the stable damage states associated with all of the random-periodic crack distributions (cf. Figs. 3 and 4) used in the numerical simulations of damage evolution. Using Eqs. (26) and (27) to describe the *sub-RVE* damage distribution, each of the Figs. 11–14 contain plots of the vector components and norm associated with the *mean mesoscale gradients of the sub-RVE damage distribution* as a function of corresponding elements of *macroscale (RVE-averaged) damage parameters* (Eqs. (5) and (7)) for the given crack configurations. A comparison of these figures reveals that the essential character of the mean mesoscale gradient versus macroscale damage relationship (i.e., distinct initial values of the components of the gradient and the trajectory of evolution) is preserved if the mean norm of the mesoscale damage gradient is used to describe the sub-RVE damage distribution. Again, an advantage of using the norm of the mesoscale gradient to characterize the fluctuation in the sub-RVE damage distribution is that the total number of higher-order ISVs is reduced and the explicit dependence of the higher-order ISVs on the choice of mesoscale coordinate system, $\hat{\boldsymbol{x}}$, is eliminated. Hence, it appears desirable to define higher-order damage ISVs based upon the mean norm of the mesoscale gradients rather than the vector components themselves.

Using the mesoscale crack density tensor (26) to depict the sub-RVE damage distribution, Figs. 11(a)–(c) show the vector components and norm, respectively, associated with the *mean mesoscale gradient*, $\nabla\hat{D}_{22}$, as a function of the *macroscale* (RVE-averaged) component of crack density tensor, D_{22}, for all the random-periodic crack distributions considered in this study. Figs. 11(a)–(c) indicate that the vector components and norm, respectively, of the *mean mesoscale gradient*, $\nabla\hat{D}_{22}$, are generally increasing functions of the *macroscale* damage parameter, D_{22}, for each crack configuration. Note that the *initial* value of the vector components and norm of the damage gradients and the evolution of the gradient terms are distinct for each of the random-periodic crack distributions. This suggests that *mean mesoscale gradients may be used to distinguish between different damage configurations that have the same value of macroscale (RVE-averaged) damage parameter*, D_{22}. In addition, Fig. 11(c) indicates that the norm of the mean mesoscale gradient, $\|\hat{\nabla}\hat{D}_{22}\|$, is a fairly *linear* function of the macroscale damage parameter, D_{22}, for each of the random-periodic crack distributions. Note that the rate of change in the norm of the mean mesoscale gradient with increasing low-order damage is nearly constant for each of the random-periodic crack distributions shown in Fig. 11(c). These key features may prove useful in formulating evolution equations for higher-order ISVs that are based the mean mesoscale gradients of damage.

Figs. 12 and 13 show the vector components and norm of the mean mesoscale gradient associated with the macroscale (RVE-averaged) components of the crack density tensor, D_{11} and D_{12}, respectively. Note that the macroscale damage parameter and corresponding components of the mean mesoscale gradient associated with the majority of the random-periodic crack distributions do not evolve appreciably from their initial values (D_{11} and D_{12} are essentially nonevolving components of the RVE-averaged crack density tensor for these cases). The component of the macroscale damage variable, D_{12}, and corresponding mesoscale damage gradients associated with random configurations (R_1) and (R_3), however, do evolve slightly from their initial values (Fig. 13). The variations in the calculated values of D_{12} and $\nabla\hat{D}_{12}$ are likely an artifact of the way the components of the macroscale and mesoscale crack density

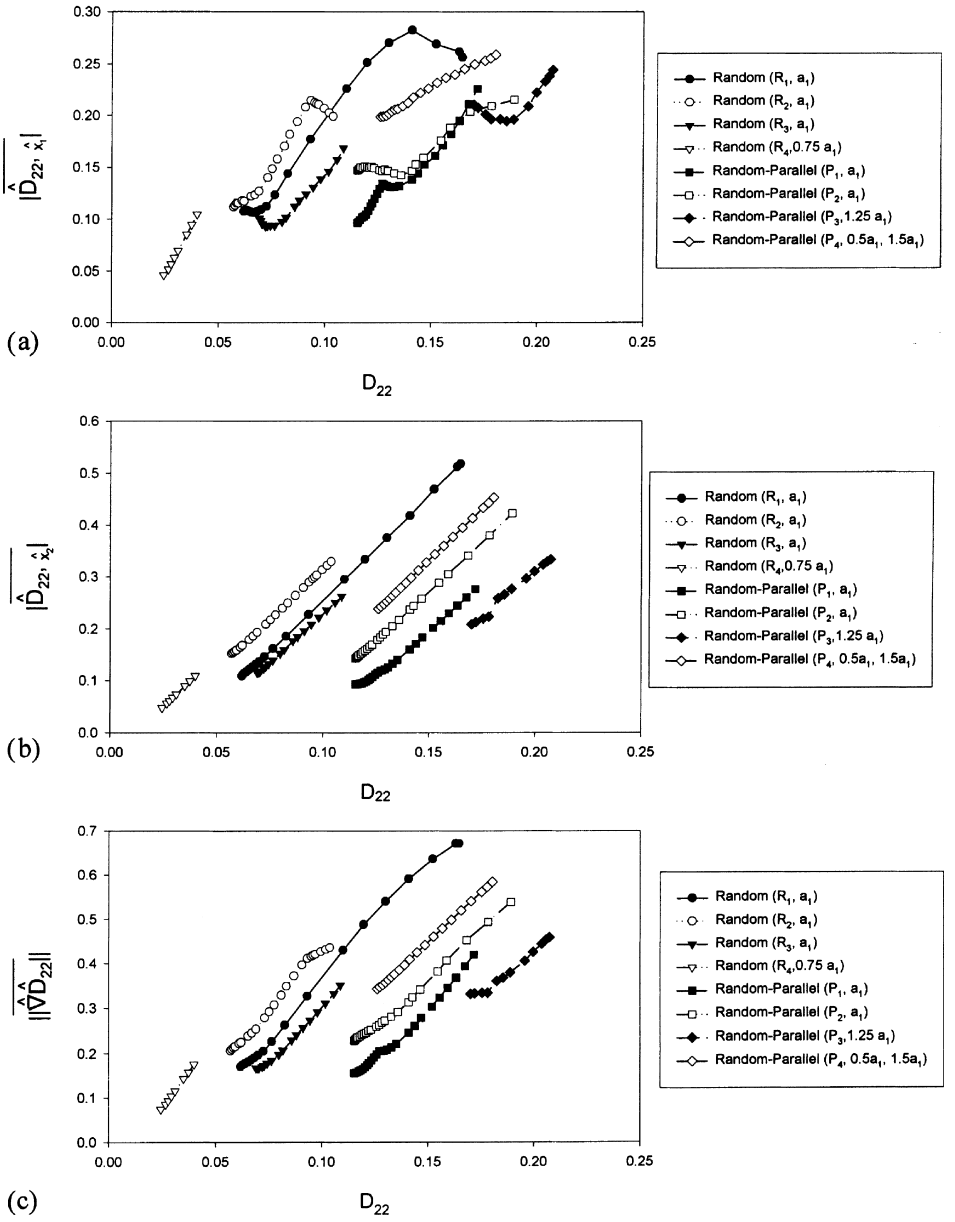

Fig. 11. (a) $\hat{x}_1$- and (b) $\hat{x}_2$-components of the mean mesoscale damage gradient; (c) mean norm of the mesoscale damage gradient ($L_{\mathrm{GRID}}/L_{\mathrm{RVE}} = 1/16,\ L_{\mathrm{SV}}/L_{\mathrm{RVE}} = 1/2$).

tensors are calculated (i.e., kinked cracks are approximated by slit cracks with identical crack tip coordinates); close inspection of the final damage states shown in Figs. 3(a) and (c) indicate that damage extension is basically normal to the direction of applied loading for each case.

Using the scalar mesoscale damage variable based on the total surface area of cracks (27) to depict the sub-RVE damage distribution, Figs. 14(a)–(c) show the vector components and norm associated with the *mean mesoscale gradient*, $\overline{\nabla \hat{D}_A}$, as a function of the corresponding *macro-*

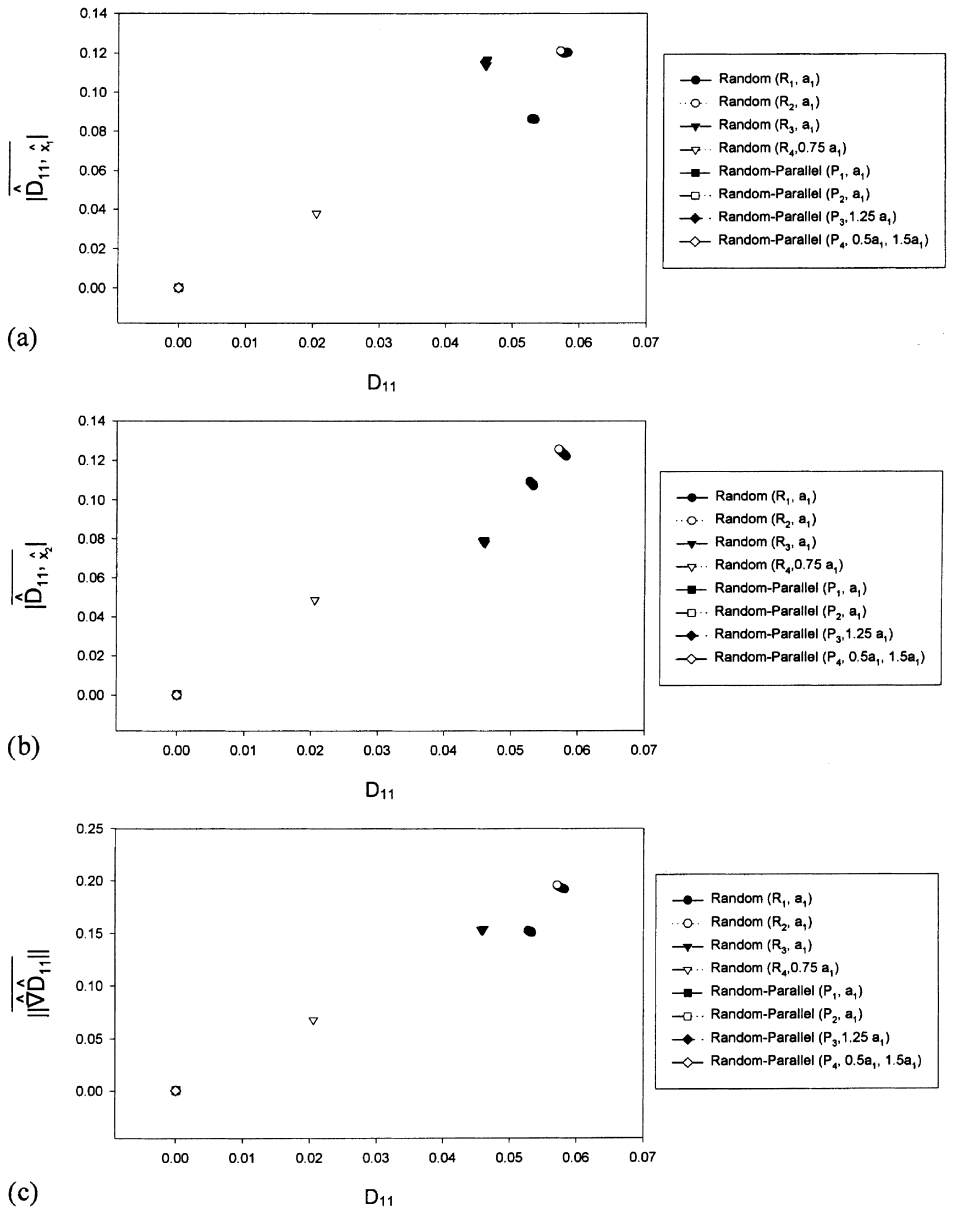

Fig. 12. (a) $\hat{x}_1$- and (b) $\hat{x}_2$-components of the mean mesoscale damage gradient; (c) mean norm of the mesoscale damage gradient ($L_{\mathrm{GRID}}/L_{\mathrm{RVE}} = 1/16,\ L_{\mathrm{SV}}/L_{\mathrm{RVE}} = 1/2$).

scale (RVE-averaged) damage parameter, D_A, for all of the considered random-periodic crack distributions. Similar to the previous case, the mean norm of the mesoscale gradient, $\|\hat{\nabla}\hat{D}_A\|$, is a fairly linear function of the macroscale damage variable, D_A, for each of the random-periodic crack distributions. Hence, it appears that, for the random-periodic crack configurations and mesoscale damage variables under consideration, use of the mean norm of the mesoscale gradient to characterize the sub-RVE damage distribution tends to smooth out any non-linear dependence

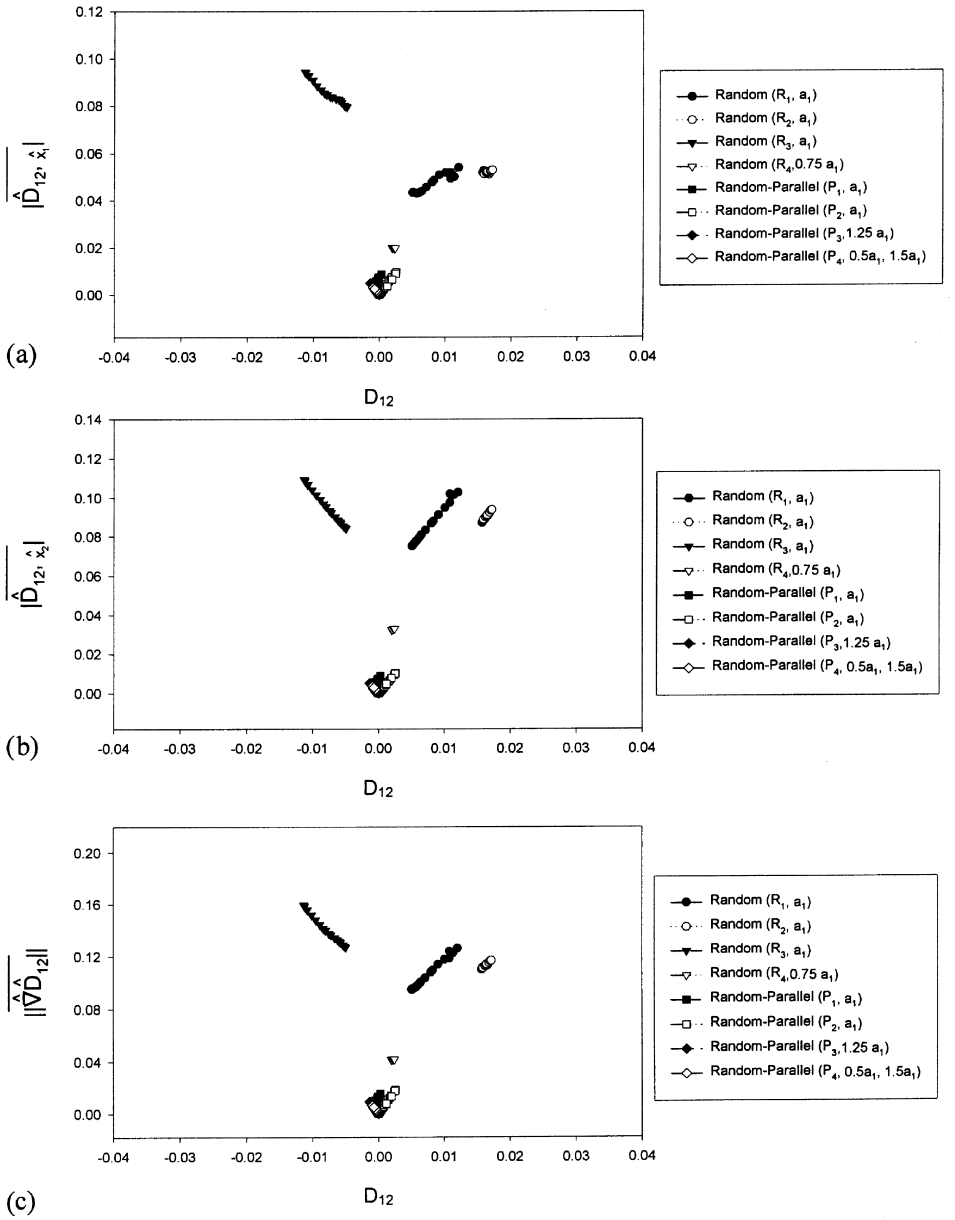

Fig. 13. (a) $\hat{x}_1$- and (b) $\hat{x}_2$-components of the mean mesoscale damage gradient; (c) mean norm of the mesoscale damage gradient ($L_{\mathrm{GRID}}/L_{\mathrm{RVE}} = 1/16,\ L_{\mathrm{SV}}/L_{\mathrm{RVE}} = 1/2$).

of the individual components of the mesoscale gradients on the macroscale damage parameter (cf. Figs. 11 and 14). Similar to the results shown in Fig. 11, the initial value of $\|\hat{\nabla}\hat{D}_A\|$ is distinct for each of the random-periodic crack distributions (cf. Fig. 14(c)).

4.4.3. Key observations based upon mesoscale gradient calculations

The preceding numerical analyses indicate that the mean norm of the mesoscale gradient of damage predicated on an overlapping subvolume averaging technique may be used to distinguish between dif-

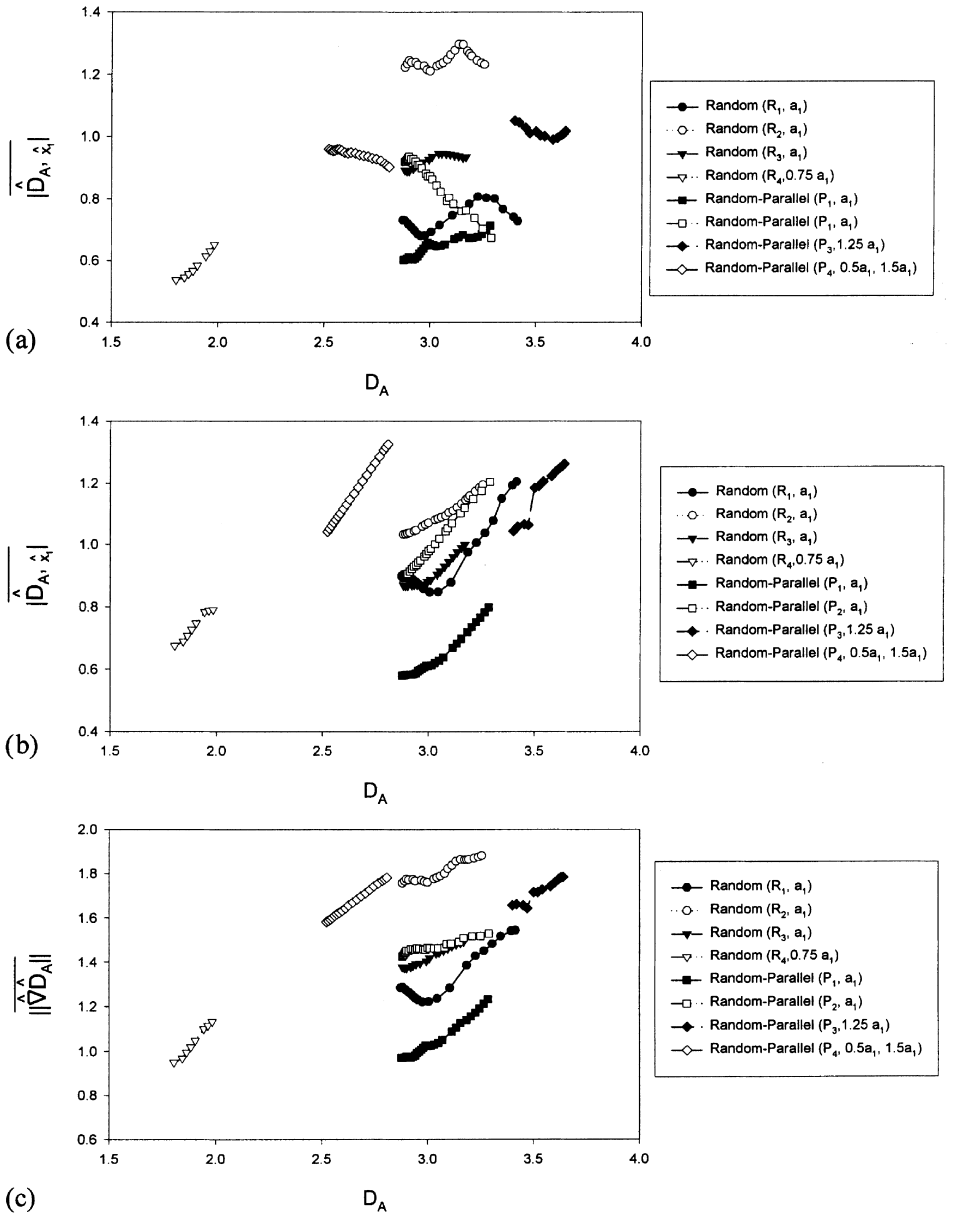

Fig. 14. (a) $\hat{x}_1$- and (b) $\hat{x}_2$-components of the mean mesoscale damage gradient based on total surface area; (c) mean norm of the mesoscale damage gradient ($L_{\mathrm{GRID}}/L_{\mathrm{RVE}} = 1/16,\ L_{\mathrm{SV}}/L_{\mathrm{RVE}} = 1/2$).

ferent distributions of defects with the same value of low-order RVE-averaged damage parameter. For the considered random periodic crack distributions, the relationships between the higher-order damage descriptors (i.e., mean norm of the mesoscale gradient, $\|\hat{\nabla}\,\hat{D}_{22}\|$ and $\|\hat{\nabla}\,\hat{D}_A\|$) and corresponding low-order damage variables (D_{22} and D_A, respectively) are, to first order, fairly linear throughout the entire range of damage evolution (Figs. 11(c), 14(c)). Thus, *the evolution of the higher-order ISVs depends only on the initial conditions of the mesoscale damage distribution*. Of course, it may

only be adopted as an hypothesis at this stage, based on limited results. If a second rank tensor is used to characterize the state of damage in a material, then the relationship between the D_{22} component of the higher-order ISV associated with mesoscale configuration and the corresponding component of the RVE-averaged damage variable may be approximated as

$$\overline{\|\hat{\nabla}\hat{D}_{22}\|} \approx a_0 + a_1 \cdot D_{22}, \tag{28}$$

where a_0 defines the initial damage state ($\|\hat{\nabla}\hat{D}_{22}\|_{\text{init}}$, $(D_{22})_{\text{init}}$) of the material and a_1 is the slope of the line defining the $\|\hat{\nabla}\hat{D}_{22}\|$ versus D_{22} relationship. The evolution equation for the higher-order ISV may be expressed in terms of the low-order ISV simply as

$$\overline{\|\hat{\nabla}\hat{D}_{22}\|}^{\cdot} \approx a_1 \cdot \dot{D}_2. \tag{29}$$

This preliminary yet promising development may facilitate the inclusion of higher-order ISVs in a CDM formulation and provides some evidence that CDM may be extended to the statistically inhomogenoeus case involving interactive damage.

Several subtle results from the numerical simulations suggest that incorporation of higher-order ISVs based on the overlapping subvolume averaging technique may eventually provide a framework for addressing the statistical inhomogeneity of the RVE-averaged ERR associated with distributions of cracks with variable size distributions. If the macroscale and mesoscale crack density tensors in Eqs. (5) and (26) are used to characterize the state of damage in a material, it appears that the initial value of the mean norm of the mesoscale gradient is sensitive to the size of defects in a given distribution. Consideration of the initial values of the mean mesoscale gradients shown in Fig. 11(c) indicates that the random-periodic distribution with the smallest initial characteristic flaw size (R_4) also had minimum initial value of $\|\hat{\nabla}\hat{D}_{22}\|$. Furthermore, the random-periodic configurations with the largest characteristic flaw sizes (P_3, P_4) had the largest initial values of $\|\hat{\nabla}\hat{D}_{22}\|$. Noting that the initial values of both the RVE-averaged ERR and the higher-order ISVs are inversely proportional to the characteristic flaw size in a given distribution (cf. Lacy et al., 1997a,b; as well as Figs. 5(b), 6(b), and 11), it is conceivable that the inclusion of higher-order ISVs in a CDM formulation may be used to sort out the differences in the RVE-averaged ERR associated with evolution of crack distributions with fundamentally different flaw sizes. It should be emphasized, however, that the aforementioned flaw size dependence manifests itself only when the macroscale and mesoscale crack density tensors in Eqs. (5) and (26) are used to characterize the damage state of the material; Fig. 14(c) shows that the initial value of the mean norm of the mesoscale gradient based on the total surface area of cracks, $\|\hat{\nabla}\hat{D}_A\|$, demonstrates no apparent flaw size dependence. Thus, $\hat{D}_A$ likely represents a poor choice of *mesoscale* damage parameter. By implication, porosity may also be inferior to other damage descriptors that appreciate the void size distribution at the mesoscale.

Recall that the numerical simulations of damage evolution were terminated when crack coalescence was imminent. While prediction of damage coalescence/localization at the mesoscale is highly desirable, it is not obvious that such events can be discerned from consideration of mean mesoscale gradients (cf. the final damage states associated with each of the curves shown in Fig. 11). This information may not manifest itself in the *extreme* values of the mesoscale gradients within the RVE ($\hat{\nabla}\hat{D}_{\text{extreme}}$) either, since there appears to be essentially no correlation between the minimum distance between flaws, $d_{\min}$, and crack extension (cf. Fig. 15). An investigation of various mesoscale coalescence criteria based upon critical values of $\hat{\boldsymbol{D}}$ is likely warranted to address this issue; such an evaluation is not considered as part of this work. Note that as cracks evolve toward coalescence, the minimum distance between flaws will decrease with increasing low-order damage (there will also be a step discontinuity in the $d_{\min}$ versus D curve at the instant of crack coalescence). This may require redefinition of L_{GRID} in order to capture coalescence events using mesoscale gradients of damage.

While the selected values of the averaging parameters L_{GRID} and L_{SV} were predicated on the assumption that the calculated gradients would reflect averaging over the zone of nonlocal action

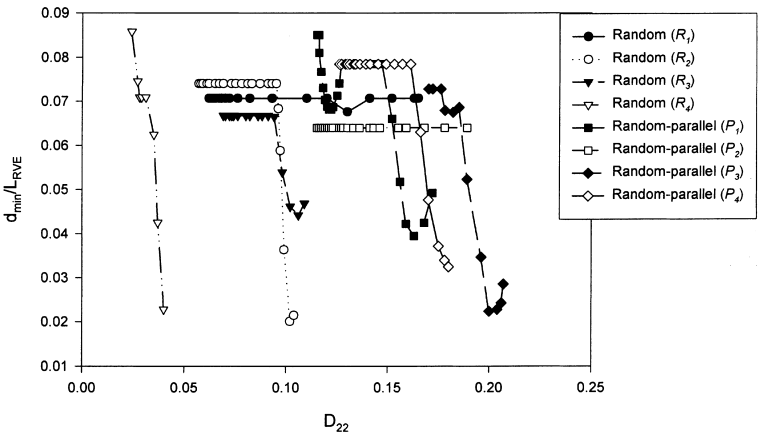

Fig. 15. Minimum nearest-neighbor distance between adjacent flaws for the random-periodic crack distributions used in numerical simulations.

associated with first nearest-neighbor crack interactions, an exhaustive study of the effect of various choices of these parameters on the calculated values of the mesoscale gradients remains to be performed. Using a subvolume grid spacing, $L_{GRID}/L_{RVE} = 0.0625$, and corresponding subvolume sizes, $L_{SV}/L_{RVE} = 0.3$, 0.5, and 0.7, respectively, Figs. 16(a)–(c) show the effect of various subvolume dimensions on the calculated values of the higher-order state variable, $\|\hat{\nabla}\hat{D}_{22}\|$, as a function of low-order damage, D_{22}. Consistent with earlier observations, increasing the subvolume dimension used in the averaging process generally lowers the magnitude of the mean mesoscale gradients. It is important to recognize, however, that the relative positions of the $\overline{\|\hat{\nabla}\hat{D}_{22}\|}$ versus D_{22} curves associated with different random-periodic crack arrays may change when the subvolume dimension is altered.

4.5. Horizons: development of a multi-scale nonlocal continuum theory

Arguably, the problem of stable microcrack evolution in initially isotropic brittle solids examined in this study may best be addressed using micromechanics. When other types of damage are considered in heterogeneous materials, however, micromechanical solutions become less tractable. In principle, the concepts outlined here may be readily applied to multi-phase materials with a wide array of damage mechanisms and may also be used to characterize the sub-RVE distribution of *stationary* (nonevolving) mesostructure; such information may prove useful in describing the distribution of potential damage nucleation sites within the RVE or when including toughening effects associated the presence of inclusions, fibers, or other second phase particles. In addition, it may be possible to experimentally quantify the initial damage states and subsequent damage evolution in various materials using high-resolution microscopy and standard stereological methods (cf. Underwood, 1970; Weibel, 1979).

The thermomechanical response of a damaged solid at a given spatial scale arguably may depend on deformation mechanisms that are manifested at that scale as well as a number of successively smaller spatial scales. The central focus of this work has been to develop the structure of a gradient theory of CDM based on multiple scales of heterogeneity up to the order of the RVE dimension. In the current formulation, inclusion of damage gradients defined at a given spatial scale arguably may be used to account for nonlocal influences at that scale; such gradients, in general, do not explicitly provide any information regarding nonlocal influences or damage localization manifested at a *higher* length scale. Thus, the effect of *mesoscale* damage gradients on nonlocal continuum behavior and damage localization at the *macroscale* is unclear.

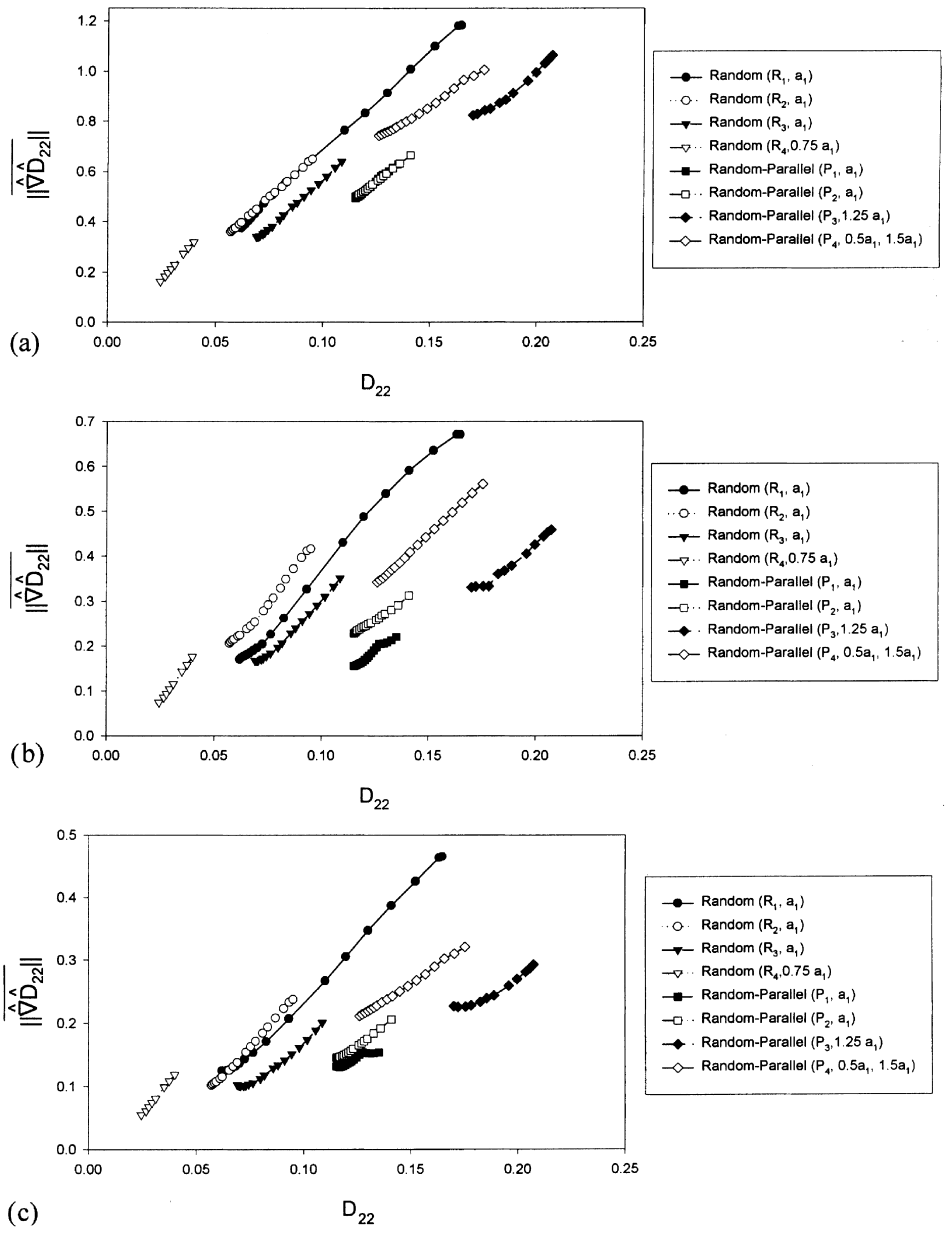

Fig. 16. Mean norm of the mesoscale damage gradient for $L_{GRID}/L_{RVE} = 1/16$. and (a) $L_{SV}/L_{RVE} = 0.3$, (b) $L_{SV}/L_{RVE} = 0.5$, and (c) $L_{SV}/L_{RVE} = 0.7$.

The inclusion of *mesoscale* gradients (or other ISVs predicated on the higher-order moments of the sub-RVE damage distribution) into a CDM formulation potentially allows for treatment of the statistical inhomogeneity of evolution associated with use of certain common damage variables; it is noted that *macroscopic* gradients are also evident in many practical applications. It is conceivable that nonlocal effects and/or damage localization may occur simultaneously at a number of different spatial scales. Thus, it may be desirable to establish a strategy for addressing

nonlocal continuum behavior at multiple scales within the framework of CDM using ISVs. In general, this may involve the inclusion of ISVs averaged over various spatial scales into the Helmholtz free energy, i.e.,

$$\psi = \psi(\boldsymbol{\varepsilon}, T, \boldsymbol{D}, \nabla \boldsymbol{D}, \overline{\hat{\nabla} \hat{\boldsymbol{D}}}). \tag{30}$$

Dependence on the gradient terms $\nabla \boldsymbol{D}$ and $\overline{\hat{\nabla} \hat{D}}$ is introduced, for illustration purposes, to account for nonlocal influences associated with nonuniformity in the damage distribution at the macroscale and mesoscale, respectively. The presence of a homogeneous damage field at a given spatial scale does not necessarily preclude nonlocal influences manifested at a fundamentally different length scale. Note that the assumption of random-periodic boundary conditions in this work ensured that there was no net flux of the mesoscale gradient across the RVE boundary; such a constraint would effectively prevent coupling between $\nabla \boldsymbol{D}$ and $\overline{\hat{\nabla} \hat{\boldsymbol{D}}}$. For sufficiently large ratio of L_{RVE} to L_{SV} (e.g., L_{SV} – extent of nonlocal action), it is likely that the net flux of $\hat{\nabla} \hat{\boldsymbol{D}}$ across the RVE boundary is suitably small to ignore. *If* it turns out that the adoption of *macroscale* gradients is meaningful (i.e., nonlocal action can occur at or in excess of the scale L_{RVE}), then they may be introduced as in other current theories (cf. Markov, 1995; Fremond and Nedjar, 1996) as evidenced in Eq. (30). Such an approach employing macroscale gradients leads to complications related to their extent of interaction; indeed, boundary conditions become an issue in this case. Clearly, employment of macroscale gradients must be subject to their scale of nonlocal action relative to mesostructure. The authors leave open the possibility that the physical basis for introduction of macroscale gradients (without introducing the distinct notions of strong interaction length scales, statistical homogeneity, or cutoff radii) is relatively undeveloped. In addition, it is not obvious that higher-order state variables averaged over different spatial scales should be independent. Further study is necessary in order to determine the role of nonlocal influences at the micro- and mesoscales on eventual damage localization at the macroscale.

5. Summary

Key issues pertaining to the development of viable damage evolution equations using a CDM approach employing low-order ISVs that can be expressed either in terms of macroscopically measurable quantities or through a spatial average of the geometric features of individual damage entities have been addressed. Implementation of either type of ISV effectively "smears out" the effect of variations in the mesostructure within the RVE; such variations play a crucial role in damage evolution and, in general, cannot be ignored. Numerical simulations of evolving random-periodic crack systems in two-dimensional perfectly brittle solids indicate that low-order damage models are inadequate in characterizing the effective moduli and damage evolution in brittle microcracked solids when the damage consists of cracks of variable size and/or spatial distributions. Statistical inhomogeneity of stiffness related response functions may arise for these crack systems when damage interactions become significant.

While a low-order CDM approach may allow for reasonably reliable estimates of elastic moduli for randomly distributed crack systems with fairly substantial crack densities, the domain of validity of such an approach to characterize damage evolution is suspect. The existence of an observation volume which is associated with SH response functions for damage evolution is by no means assured for a given selection of damage parameter. Use of certain low-order damage variables leads to response functions related to evolution that have an intrinsic flaw size dependence. Hence, damage evolution in this case is an inherently statistically inhomogeneous process. Application of CDM to the statistically inhomogeneous case is problematic, but may minimally require the introduction of additional ISVs that account for the effect of the sub-RVE damage configuration on the macroscale response.

An argument for implementing ISVs based on higher-order moments of the damage distribution within the RVE used for stiffness determination has been presented. A form for higher-order ISVs based upon the gradient of the mesoscale damage distribution has been proposed. An approximate

method has been suggested for calculating the mean gradient of the mesoscale damage distribution using an overlapping RVE subvolume averaging procedure involving two nonlocal length scales corresponding to the subvolume dimension and grid spacing, respectively, used in the averaging process. While the selection of optimum length scales for mesoscale averaging requires further study, it seems reasonable that such dimensions should be predicated on key features of the crack array geometry (minimum tip-to-tip distance, mean crack spacing, etc.), characteristic material dimensions (mean grain size, fiber diameter, etc.), or other lengths linked to the extent of nonlocal influence within the mesostructure.

The introduction of the mesoscale gradient concept in this work suggests (at least) two important length scales: (i) a subvolume scale associated with strong nearest and second nearest-neighbor interactions of highly nonlocal character, and (ii) the RVE scale of sufficient size to warrant (in some cases) SH properties or evolution of properties within. Through the introduction of these two scales and the notion of RVE-averaged mean mesoscale gradient of damage, a "cutoff" scale for the extent of nonlocal action ($\sim L_{SV}$) is effectively introduced by adopting a local formulation at the RVE scale.

The higher-order state variables were calculated for every stable damage state associated with each of the random-periodic crack configurations considered in this study. In each case, the higher-order ISVs were distinct functions of corresponding low-order damage ISVs. Hence, the higher-order ISVs were able to distinguish between different mesoscale damage configurations leading to the same value of low-order damage parameter. Furthermore, the mean norm of the mesoscale gradient of damage for the cases considered was a reasonably linear function of the corresponding low-order damage variable. This potentially allows for the formulation of fairly elementary evolution equations for the higher-order ISVs. While still preliminary and requiring further development, use of higher-order ISVs based on the mesoscale gradients of damage may provide a framework for extending CDM to the statistically inhomogeneous case involving interactive damage.

Acknowledgements

This work was made possible by the award of NASA fellowship NGT-51178 to T.E. Lacy. In addition, use of Cornell University's/Kansas State University's special purpose finite element code, FRANC2D/L, in our numerical calculations was greatly appreciated. D.L. McDowell is grateful to the ARO Solid Mechanics Program (Dr. K. Iyer, monitor) for support.

References

Aifantis, E.C., 1992. On the role of gradients in the localization of deformation and fracture. Int. J. Engng. Sci. 30, 1279.

Aifantis, E.C., 1994. Spatio-temporal instabilities in deformation and fracture. In: Noor, A.K., Needleman, A. (Eds.), AD-Vol. 42/PVP-Vol. 294, Computational Material Modeling, ASME, New York, p. 199.

Aifantis, E.C., 1995. Pattern formation in plasticity. Int. J. Engng. Sci. 33, 2161.

Alzebdeh, K., Jasiuk, I., Ostoja-Starzewski, M., 1997. Scale and boundary conditions effects in elasticity and damage mechanics. In: Ju, J.W., Chaboche, J.-L., Voyiadjis, G. (Eds.), Damage Mechanics, Studies in Applied Mechanics, in press.

Andrieux, S., Joussemet, M., Lorentz, E., 1996. A class of constitutive relations with internal variable derivatives from homogenization and initial value problem. Journal de Physique IV Colloque C6, supplement au Journal de Physique III 6, C6–463.

Annigeri, B.S., Cleary, M.P., 1984. Surface integral finite element hybrid (SIFEH) method for fracture mechanics. Int. J. Numer. Methods Engng. 20, 869.

Bazant, Z.P., 1994. Nonlocal damage theory based on micromechanics of crack interactions. J. Engng. Mech. 120 (3), 593 (with Errata and Addendum in No. 6, 1401).

Bazant, Z.P., Chen, E.-B., 1997. Scaling of structural failure. ASME Appl. Mech. Rev. 50, 593.

Binienda, W.K., Arnold, S.M., Tan, H.Q., Xu, M.H., 1993. Stress intensity factors in a fully interacting, multicracked, isotropic plate. Comput. Mech. 12, 297.

Bittencourt, T.N., Wawrzynek, P.A., Sousa, J.L., 1996. Quasi-automatic simulation of crack propagation for 2D LEFM problems. Engrg. Fract. Mech. 55, 321.

Boyd, J.G., 1992. A micropolar damage model for brittle matrix composites. In: Allen, D.H., Lagoudas, D.C. (Eds.), Damage Mechanics in Composites, AMD-Vol. 150, AD-Vol. 32, ASME, p. 295.

Brebbia, C.A., Telles, J.C.F., Wrobel, L.C., 1984. Boundary Element Techniques. Springer, Berlin.

Budiansky, B., O'Connell, R.J., 1976. Elastic moduli of a cracked solid. Int. J. Solids Struct. 12, 81.

Chaboche, J.-L., 1984. Anisotropic creep damage in the framework of continuum damage mechanics. Nuc. Engng. Design 79, 309.

Coleman, B.C., Gurtin, M., 1967. Thermodynamics with internal state variables. J. Chem. Phys. 47, 597.

Costanzo, F., Boyd, J.G., Allen, D.H., 1996. Micromechanics and homogenization of inelastic composite materials with growing cracks. J. Mech. Phys. Solids 44, 333.

Edelen, D.G.B., 1976. Nonlocal field theories. In: Eringen, A.C. (Ed.), Continuum Physics Volume IV – Polar and Nonlocal Field Theories. Academic Press, New York, p. 75.

Eringen, A.C., 1966. A unified theory of thermomechanical materials. Int. J. Engng. Sci. 4, 179.

Fremond, M., Nedjar, B., 1996. Damage, gradient of damage and principle of virtual power. Int. J. Solids Struct. 33, 1083.

Germain, P., Nguyen, Q.S., Suquet, P., 1983. Continuum thermodynamics. J. Appl. Mech. 50, 1010.

Gokhale, A.M., 1996. Estimation of bivariate size and orientation distribution of microcracks. Acta Mater. 44, 475.

Hashin, Z., 1983. Analysis of composite materials – A survey. J. Appl. Mech. 50, 481.

Hill, R., 1967. The essential structure of constitutive laws for metal composites and polycrystals. J. Mech. Phys. Solids 15, 79.

Hoffman, J.D., 1992. Numerical Methods for Engineers and Scientists. McGraw-Hill, New York, USA.

James, M., Swenson, D., 1997. FRANC2D/L: A Crack Propagation Simulator for Plane Layered Structures, available from http://www.mne.ksu.edu/~franc2d/.

Kachanov, L.M., 1958. On the creep rupture time. Izv. A.N. SSSR Otd., Tekhn. Nauk. 8, 26.

Kachanov, M., 1980. A continuum model of medium with cracks. J. Engng. Mech. 106, 1039.

Kachanov, M., 1987. Elastic solids with many cracks: A simple method of analysis. Int. J. Solids Struct. 23, 23.

Kachanov, M., 1992. Effective elastic properties of cracked solids: Critical review of some basic concepts. Appl. Mech. Rev. 45, 304.

Kachanov, M., 1994. Elastic solids with many cracks and related problems. Adv. in Appl. Mech. 30, 259.

Kestin, J., 1966. On the application of the principles of thermodynamics to strained solid materials. In: Parkus, H., Sedov, L.I. (Eds.), Irreversible Aspects of Continuum Mechanics, and Transfer of Physical Characteristics in Moving Fluids. Springer, New York, p. 177.

Kestin, J., Rice, J.R., 1970. Paradoxes in application of thermodynamics to strained solids. In: Stuart, E.B., Brainard, A.J., Gal-Or, B. (Eds.), A Critical Review of Thermodynamics. Mono Book Corporation, Baltimore, MD, p. 275.

Krajcinovic, D., 1989. Damage mechanics. Mech. Mater. 8, 117.

Krajcinovic, D., 1996a. Damage Mechanics. Elsevier, Amsterdam.

Krajcinovic, D., 1996b. Essential structure of the damage mechanics theories. In: Tatsumi, T., Watanabe, E., Kambe, T. (Eds.), Theoretical and Applied Mechanics. Elsevier, Amsterdam, p. 411.

Kroner, E., 1967. Elasticity theory of materials with long range cohesive forces. Int. J. Solids Struct. 3, 731.

Lacy, T.E., 1998. Distribution effects in damage mechanics. Ph.D. Thesis, Georgia Institute of Technology, Atlanta, GA.

Lacy, T.E., McDowell, D.L., Willice, P.A., Talreja, R., 1997a. On representation of damage evolution in continuum damage mechanics. Int. J. Damage Mech. 6, 62.

Lacy, T.E, McDowell, D.L., Talreja, R., 1997b. Effects of damage distribution on evolution. In: McDowell, D.L. (Ed.), Applications of Continuum Damage Mechanics to Fatigue and Fracture, ASTM STP 1315. American Society for Testing and Materials, p. 131.

Markov, K.Z., 1995. On a microstructural model of damage in solids. Int. J. Engng Sci. 33, 139.

Mulhaus, H.-B., Aifantis, E.C., 1991. A variational principle for gradient plasticity. Int. J. Solids Struct. 28, 845.

Mura, T., 1991. Micromechanics of Defects in Solids, 2nd ed. M. Nijhoff Publ., The Hague.

Nemat-Nasser, S., Hori, M., 1993. Micromechanics: Overall Properties of Heterogeneous Materials. North-Holland, Amsterdam.

Onat, E.T., Leckie, F.A., 1988. Representation of mechanical behavior in the presence of changing internal structure. J. Appl. Mech. 55, 1.

Ostoja-Starzewski, M., 1997. Random fields models of heterogeneous materials. Int. J. Solids Struct. 35, 2429.

Ostoja-Starzewski, M., Sheng, P.Y., Jasiuk, I., 1994. Influence of random geometry on effective properties and damage formation in composite materials. J. Engng. Mat. Tech. 116, 384.

Ostoja-Starzewski, M., Wang, C., 1989. Linear elasticity of planar Delaunay networks: Random field characterization of effective moduli. Acta Mech. 80, 61.

Peerlings, R.H.J., DeBorst, R., Brekelmans, W.A.M., De Vree, J.H.P., 1996. Gradient enhanced damage for quasi-brittle materials. Int. J. Numer. Methods Engng. 39, 3391.

Pijaudier-Cabot, G., Bazant, Z.P., 1987. Nonlocal damage theory. J. Engng. Mech. 113, 1512.

Pyrz, R., 1994. Correlation between microstructure variability and local stress field in two-phase materials. Mater. Sci. Engng. A 177, 253.

Rabotnov, Y.N., 1963. On the equations of state for creep. In: Progress in Applied Mechanics, the Prager Anniversary Volume. Macmillan, New York, NY, p. 307.

Rice, J.R., 1971. Inelastic constitutive relations for solids: An internal-variable theory and its application to metal plasticity. J. Mech. Phys. Solids 19, 433.

Ripley, B.D., 1981. Spatial Statistics. Wiley, New York.

Sanchez-Palencia, E., Zaoui, A., 1987. Homogenization Techniques for Composite Media. Springer, Berlin.

Stoyan, D., Kendall, W.S., Mecke, J., 1987. Stochastic Geometry and Its Applications. Wiley, New York.

Stoyan, D., Stoyan, H., 1994. Fractals, Random Shapes and Point Fields, Methods of Geometrical Statistics. Wiley, New York.

Talreja, R., 1989. Damage development in composites: Mechanisms and modelling. J. Strain Anal. 24, 215.

Talreja, R., 1991. Continuum modeling of damage in ceramic matrix composites. Mech. Mater. 12, 165.

Underwood, E.E., 1970. Quantitative Stereology. Addison-Wesley, Reading, MA.

Vakulenko, A.A., Kachanov, M., 1971. Continual theory of a medium with cracks. Izv. AN SSSR., Mekhanika Tverdogo Tela (Mech. Solids) 6 (4), 159.

Weibel, E.R., 1979. Stereological Methods, vols. 1 & 2. Academic Press, London.